Phytochemistry Reviews **2:** 257–288, 2003.

An historical perspective on lignan biosynthesis: Monolignol, allylphenol and hydroxycinnamic acid coupling and downstream metabolism

Laurence B. Davin & Norman G. Lewis*
Institute of Biological Chemistry, Washington State University, 467 Clark Hall, Pullman, WA 99164-6340, U.S.A.;
**Author for correspondence (Tel: 509-335-8382; Fax: 509-335-8206; E-mail: lewisn@wsu.edu)*

Key words: aryl propenal double bond reductase, dirigent proteins, enantiospecificity, lignans, phenylcoumaran benzylic ether reductase, pinoresinol-lariciresinol reductase, polyphenol oxidase, radical-radical coupling, regiospecificity, secoisolariciresinol dehydrogenase, stereoselective coupling

Abstract

This review describes discoveries from this laboratory on monolignol, allylphenol and hydroxycinnamic acid coupling, and downstream metabolic conversions, affording various lignan skeleta. Stereoselective 8–8′ coupling (dirigent protein-mediated) of coniferyl alcohol to afford (+)-pinoresinol is comprehensively discussed, as is our current mechanistic/kinetic understanding of the protein's radical-radical binding, orientation and coupling properties, and insights gained for other coupling modes, e.g. affording (−)-pinoresinol. In a species dependent manner, (+)- or (−)-pinoresinols can also undergo enantiospecific reductions, catalyzed by various bifunctional pinoresinol-lariciresinol reductases (PLR), to afford lariciresinol and then secoisolariciresinol. With X-ray structures giving a molecular basis for differing PLR enantiospecificities, comparisons are made herein to the X-ray structure of the related enzyme, phenylcoumaran benzylic ether reductase, capable of 8–5′ linked lignan regiospecific reductions. Properties of the enantiospecific secoisolariciresinol dehydrogenase (also discovered in our laboratory and generating 8–8′ linked matairesinol) are summarized, as are both *in situ* hybridization and immunolocalization of lignan pathway mRNA/proteins in vascular tissues. This entire 8–8′ pathway thus overall affords secoisolariciresinol and matairesinol, viewed as cancer preventative agent precursors, as well as intermediates to cancer treating substances, such as podophyllotoxin derivatives. Another emphasis is placed on allylphenol/hydroxycinnamic acid coupling and associated downstream metabolism, e.g. affording the antiviral creosote bush lignan, nordihydroguaiaretic acid (NDGA), and the fern lignans, blechnic/brainic acids. Regiospecific 8–8′ allylphenol coupling is described, as is characterization of the first enantiospecific membrane-bound polyphenol oxidase, (+)-larreatricin hydroxylase, involved in NDGA formation. Specific [^{13}C]-labeling also indicated that *Blechnum* lignans arise from stereoselective 8–2′ hydroxycinnamic acid coupling.

Abbreviations: CD – circular dichroism; e.e. – enantiomeric excess; DP – dirigent protein; ESI-MS – electrospray ionization mass spectrometry; MALDI -TOF – matrix assisted laser desorption ionization-time of flight; MALLS – multiangle laser light scattering; PLR – pinoresinol lariciresinol reductase; SDH – secoisolariciresinol dehydrogenase.

Introduction

Our scientific interests and reports of lignan formation *in planta* began in the nineteen-eighties (Pullockaran et al., 1989) for several reasons. Firstly, the discoveries by other workers of the quite remarkable biological properties of lignans in human health protection and medicine (Hartwell and Schrecker, 1951, 1958; Kelly and Hartwell, 1954; MacRae and Towers, 1984) as well as in plant defense (Clark et al., 1981; Taniguchi et al., 1989) were of considerable significance. A second reason for interest involved several intriguing reports which suggested, but did not prove, that cer-

tain lignans might be pathway intermediates to the polymeric cell-wall structural components, the lignins (Dewick, 1990). Thirdly, many lignans of widely differing skeletal types were reported to be optically active (but not necessarily optically pure), whereas others were racemic and/or near racemic, suggesting unique and/or distinct mechanisms of coupling. [Note that while lignans generally exist as phenylpropanoid dimers, higher oligomers are also found, with the largest reported thus far having a MW of *circa* 10,000 Da in western red cedar (Johansson et al., 2000).]

Our initial research goals mainly encompassed two topics: (i) to define the underlying biochemical mechanisms affording the varied and often complex skeleta found in this large class of natural products and what the relationship was, if any, to lignin assembly (summarized below) (Davin and Lewis, 1992; Lewis et al., 1998, 1999; Lewis and Davin, 1999) and (ii) to understand further the reasons for the emerging roles of lignans (involving structural diversification) during evolution of land-based vascular plants (Lewis and Davin, 1994; Lewis et al., 1995).

This contribution briefly touches upon both the evolutionary aspects of lignan occurrence, which are well documented elsewhere (Lewis and Davin, 1994, 1999; Lewis et al., 1995) and that of the reasoning for our preferred lignan nomenclature. In terms of evolutionary patterns, lignans are apparently absent in algae but are present in 'primitive' early land plants, such as the liverworts *Pellia epiphylla* (Cullmann et al., 1993, 1996) and *Jamesoniella autumnalis* (Tazaki et al., 1995), these containing the presumed caffeic acid (**1**) derived compounds, **2**–**5** and **6**–**11**, respectively (Scheme 1). Lignans are also widely distributed in the Pteridophytes, such as the 8–5′ and 8–8′ linked glucosides of (−)-dihydrodehydrodiconiferyl alcohol (**12**) and (+)-lariciresinol (**13**) in *Pteris vittata* (Li et al., 1997; Satake et al., 1978), whose lignan components are considered derived from coniferyl alcohol (**14**). Interestingly, some other ferns, such as *Blechnum orientale* (Wada et al., 1992) and *B. spicant* (Davin et al., 2003; Wang et al., 2001) accumulate other presumed caffeic acid (**1**) derived lignans, i.e. the 8–2′-linked (−)-blechnic (**16**) and (−)-brainic (**17**) acids. Additionally, from *Selaginella doedeleinii* in the Lycopsida, a variety of lignans are present including (+)-*nor*-trachelogenin (wikstromol) (**18**) and (−)-syringaresinol [(−)-lirioresinol B] (**19**) (Lin et al., 1994). The latter is of particular interest from an evolutionary perspective, since syringaresinol (**19**) moieties are normally considered to have evolved in the angiosperms, [i.e. via coupling of sinapyl alcohol (**15**) (Lewis and Yamamoto, 1990)] rather than being present in earlier plant forms.

In contrast to what little is currently known about early land plant lignans, the gymnosperms were evolutionarily accompanied by a massive increase in lignan structures (Lewis and Davin, 1994; Lewis et al., 1995), most of which are 8–8′ linked and coniferyl alcohol (**14**) derived, such as plicatic acid (**20**, Scheme 2) and its derivatives (Fujita et al., 1999; Gardner et al., 1960, 1966; Kim et al., 2002a, 2002b). However, 8–5′ and 8–*O*–4′ linked lignans, e.g. (±)-dehydrodiconiferyl alcohols (**21a/b**) and (±)-*erythro/threo* guaiacylglycerol 8–*O*–4′ coniferyl alcohol ethers (**22a/b**) are widespread as well, these also being coniferyl alcohol (**14**) derived (Schemes 1 and 2) (Croteau et al., 2000; Gang et al., 1999b; Lewis and Davin, 1994, 1999; Nose et al., 1995).

In a somewhat similar manner, the transition to angiosperms was also accompanied by a massive increase in lignan structural types/new skeletal forms. While again the prevalent linkage reported thus far is that of 8–8′ for both monolignol (Davin et al., 1992; Gang et al., 1997; Lewis and Davin, 1992, 1998, 1999) and allylphenol-derived lignans (Cho et al., 2003; Lewis and Davin, 1999; Moinuddin et al., 2003), other linkages such as 8–1′, 8–5′, 5–5′, 7–1′, 8–7′, 1–5′, 8–*O*–4′, 2–*O*–3′ and 3–*O*–4′ also emerged – particularly in the Magnoliiflorae (Gottlieb, 1972, 1978; Gottlieb and Yoshida, 1989; Lewis and Davin, 1994; Nascimento et al., 2000). Additionally, monocots often contain cyclobutane lignan dimers, including metabolites such as the dihydroxytruxillic acids **23** and **24** present in *Sataria anceps* cv Nandi (Poaceae, Commeliniflorae) (Ford and Hartley, 1990; Hartley and Ford, 1989) and acoradin (**25**) from *Acorus calamus* (Araceae, Ariflorae) (Patra and Mitra, 1979). Indeed, from the analysis and classification of existing chemotaxonomic data, together with the recently discovered lignan biochemical pathways, it is now possible – with a high level of probability – to predict lignan structural variants in specific plant family superorders (Lewis et al., 1995).

Lignan nomenclature

In terms of lignan nomenclature, it is our consideration that the term lignan should solely be used to encompass all skeletal types, whether monolignol, allylphenol or hydroxycinnamic acid derived (Lewis

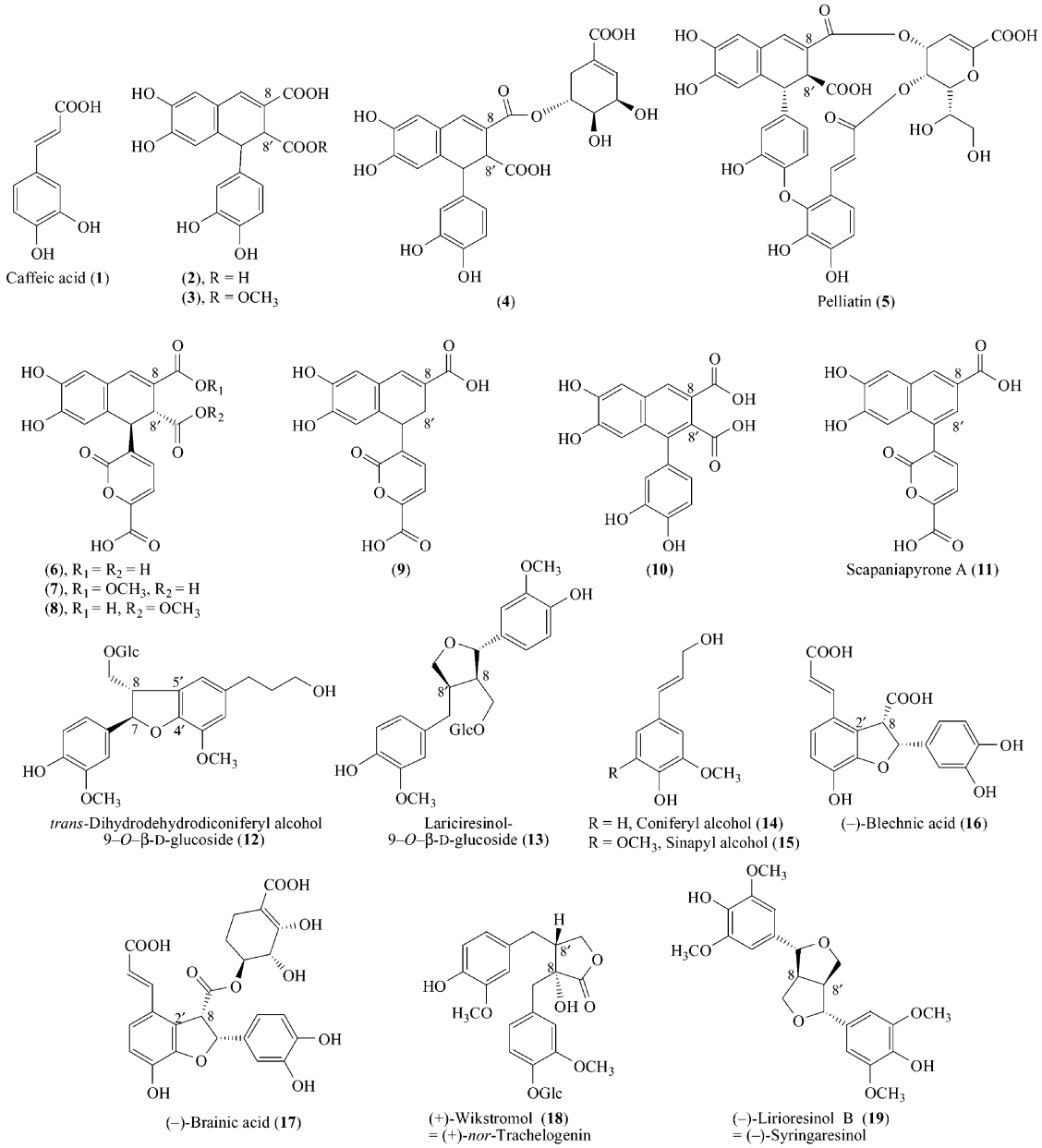

Scheme 1. Representative examples of different lignan skeleta and monolignols/hydroxycinnamic acids.

and Davin, 1999). This is because, irrespective of molecular size (dimers, trimers and higher oligomers, etc.), there are only a relatively small number of phenylpropanoid interunit linkages, and these can be conveniently and precisely stipulated, e.g. 8–8′, 8–1′, 8–5′, 8–*O*–4′, 5–5′, 3–*O*–4′, 7–1′, 8–7′, 1–5′, 2–*O*–3′, etc. Adoption of this nomenclature would eliminate the need for terminologies (such as neolignans) to describe either distinct linkage types (i.e. non 8–8′) and/or of those derived from non-monolignol (e.g., allylphenol) origin.

Lignan biosynthetic pathway studies: organization and scope of review

As regards the biosynthetic pathways to the lignans, essentially little was known at the onset of our investigations, although some preliminary tracer studies had been carried out (Jackson and Dewick, 1984; Kamil

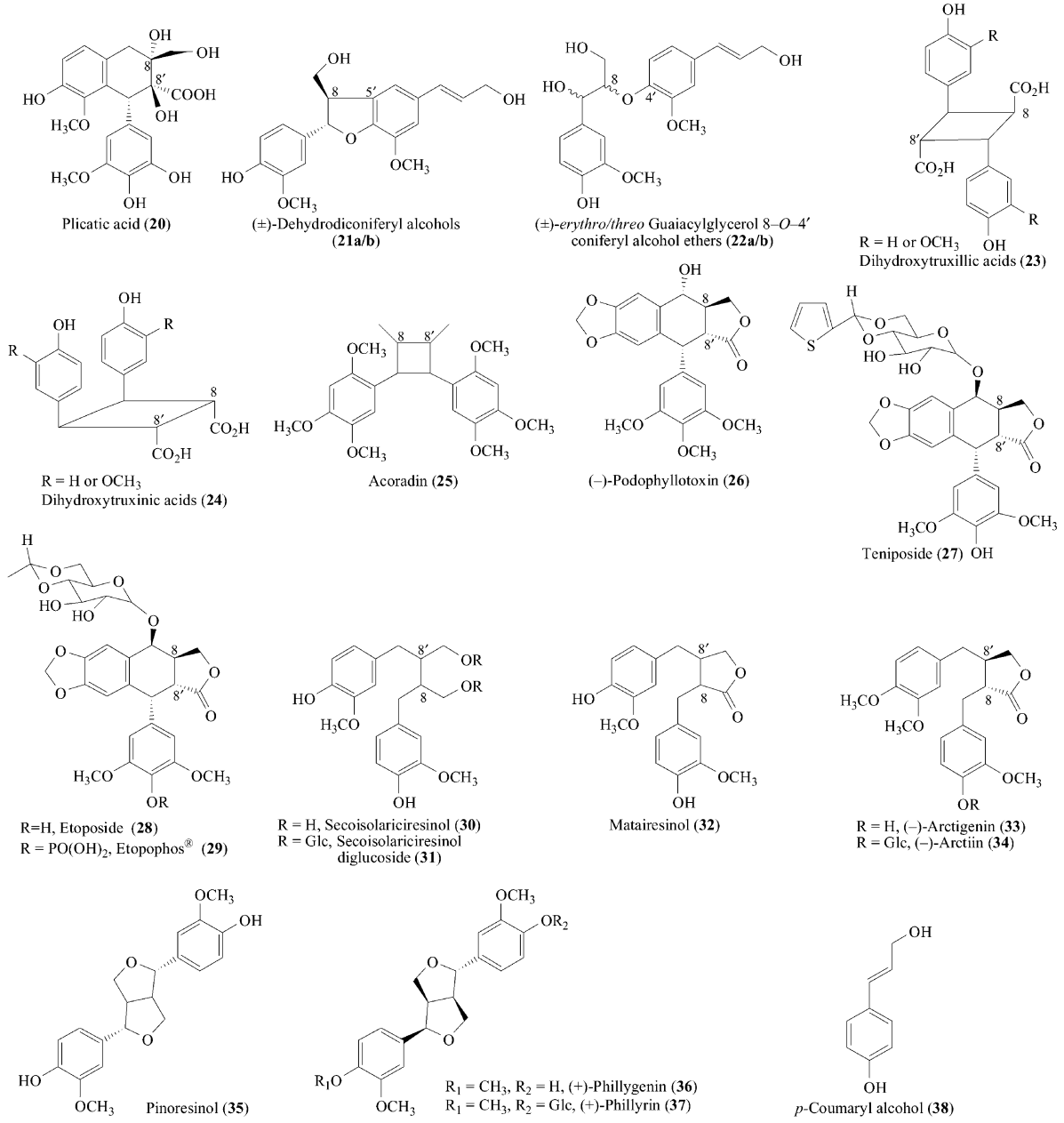

Scheme 2. Selected lignans from gymnosperms and angiosperms, semi-synthetic derivatives of podophyllotoxin (**26**) and the monolignol *p*-coumaryl alcohol (**38**).

and Dewick, 1986; Stöckigt and Klischies, 1977). Hence, we considered that it would be instructive to comprehensively investigate how such substances were formed (i.e. including fully defining biochemical steps, enzymes, proteins and genes involved).

Organizationally, we attempt to provide a historical perspective of our studies over the last fifteen years or so on lignan formation *in planta* to the present date, with related work discussed as needed. It begins with *in vivo* tracer labeling studies and potential substrate metabolism studies in crude extracts from *Forsythia* species, and the insights into both stereoselective coupling and accompanying stereo- and enantiospecific transformations that resulted from these investigations. From these beginnings, it was possible to next target the proteins (and encoding genes involved),

and to establish in most cases tissue and cellular locations of these proteins and/or their patterns of gene expression. A more recent emphasis has been placed on obtaining a full mechanistic understanding of the biochemical processes involved for each transformation, including determining the three-dimensional structures of various proteins and enzymes using X-ray crystallography. Note also that in our studies, the lignans of initial interest included the antiviral lignan, podophyllotoxin (**26**), whose derivatives teniposide (**27**), etoposide (**28**) and etopophos® (**29**), are widely used in cancer treatments, e.g. Hodgkin's and non-Hodgkin's lymphoma, testicular/small cell lung cancers and acute leukemia (Droz and Rivoire, 2001; Glossmann et al., 2002; Hainsworth, 1999; Hande, 1998; Nichols, 2001; Pasini et al., 2002; Sandler, 2003), as well as that of secoisolariciresinol (**30**) (diglucoside (**31**)) and matairesinol (**32**), widely reported to provide chemo-protection to mammals against the onset of various cancers, such as breast, prostate and colorectal (Thompson, 1998). Other interests involved lignans that are deposited during heartwood formation, e.g., plicatic acid (**20**) and its analogs in western red cedar (*Thuja plicata*) (Gardner et al., 1960; Gardner et al., 1966) and the 8–5′ moieties present in pine species, e.g., dehydrodiconiferyl alcohol (**21**) in loblolly pine (*Pinus taeda*) (Nose et al., 1995).

Tracer studies and investigations with cell-free extracts from *Forsythia* species: Advantages and limitations as to their utility in identifying both monomeric moieties undergoing coupling and associated downstream lignan metabolism

In the late nineteen-eighties/early nineteen-nineties, we began to conduct a number of potential precursor administration experiments, together with examining the metabolism of possible substrates in cell-free extracts, using *Forsythia* species. This was in order to begin to probe the biosynthetic pathways to its major lignans, which included in *Forsythia intermedia*, the (−)-antipode of matairesinol (**32**), (−)-arctigenin (**33**) and (−)-arctiin (**34**), and in *F. suspensa*, (+)-pinoresinol (**35**), (+)-phillygenin (**36**) and (+)-phillyrin (**37**) (Nishibe et al., 1988). Prior to these studies, there was no compelling evidence as to whether entry into this pathway involved initial monolignol [e.g., coniferyl alcohol (**14**)] coupling, followed by further metabolism, or whether hydroxycinnamic acids, hydroxycinnamaldehydes and/or mixed substrate coupling modes were in effect.

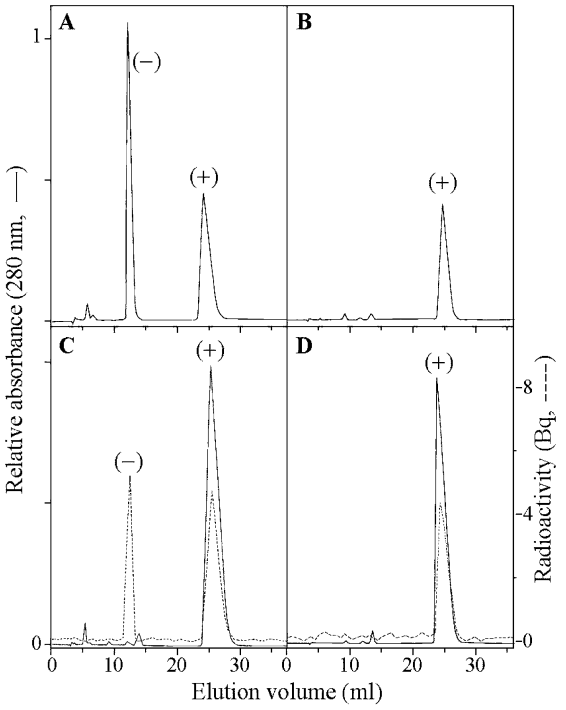

Figure 1. HPLC chiral separations of purified pinoresinols in racemic (**35a/b**) or enantiomerically pure (**35a**) form. (**A**) (±)-Pinoresinols (**35a/b**) obtained following horseradish peroxidase/H_2O_2 treatment of coniferyl alcohol (**14**), (**B**) (+)-pinoresinol (**35a**) from *F. suspensa*, (**C**) UV and radiochromatograms of pinoresinols (**35a/b**) isolated from *F. suspensa* following [8-^{14}C]coniferyl alcohol (**14**) administration to excised shoots for 3 hours and (**D**) UV and radiochromatograms of (+)-pinoresinol (**35a**) isolated from *F. suspensa* following [U-^{14}C]phenylalanine administration to excised shoots for 3 h. Redrawn from Umezawa, Davin, Kingston, Yamamoto and Lewis (1990b).

Our first insight into the nature of the initial lignan coupling product was obtained following administration of [U-^{14}C]Phe to *F. suspensa* shoots for periods of 3, 9 and 24 h, respectively. These experiments established that [U-^{14}C]Phe was apparently only converted into (+)-pinoresinol (**35a**), since the (−)-antipode (**35b**) was not detected, as determined using chiral HPLC analysis (see Figure 1A for separation of synthetic (+)- and (−)-antipodes (**35a/b**) and Figure 1D for [^{14}C] labeling of only (+)-pinoresinol (**35a**), respectively); structures are depicted in Figure 2 (Davin et al., 1990, 1992; Umezawa et al., 1990b). This finding was further supported by isolation of pinoresinol (**35**) from *F. suspensa* stems (shoots) which also established, based on HPLC chiral column analysis, that only the (+)-antipode **35a** was detectable (Figure 1B).

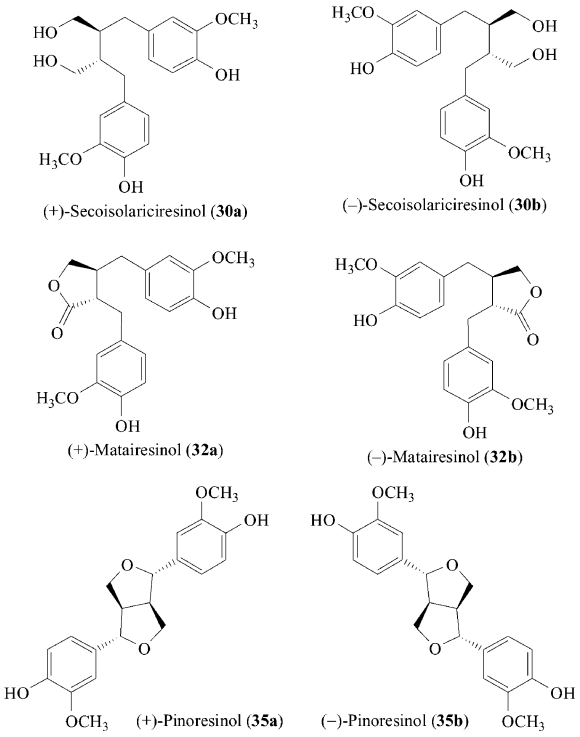

Figure 2. Antipodes (+ and −) of lignans **30**, **32** and **35**.

It is noteworthy, however, that when [8-^{14}C]coniferyl alcohol (**14**) was administered to *F. suspensa* shoots in the same manner (for 3, 9 and 24 h), both (+)- and (−)-antipodes of pinoresinol (**35a/b**) were radiolabeled (i.e. in an ∼6:4 ratio at 3 h, Figure 1C), with the (+)-antipode (**35a**) later becoming preferentially labeled by 24 h (ratio of **35a/b**, 9:1). We interpreted this data, when using [8-^{14}C]coniferyl alcohol (**14**) as a potential precursor, as a consequence of a lack of specificity in coupling and inadequate (improper) metabolite compartmentation. On the other hand, the Phe administration data suggested proper metabolic channeling into the appropriate compartment with stereoselective coupling then occurring to give (+)-pinoresinol (**35a**). Nevertheless, while these findings using [U-^{14}C]Phe were most encouraging, it was not possible to determine whether stereoselective coupling had indeed occurred in *F. suspensa*, or whether the (−)-antipode of pinoresinol (**35b**) was being selectively depleted.

Lignan biogenesis in *F. intermedia* was next addressed, since this species accumulates arctigenin (**33**) and arctiin (**34**), both potentially being derived from secoisolariciresinol (**30**) and matairesinol (**32**). Individual administrations and uptake of [8-^{14}C] and [9-$^{2}H_2$, OC$^{2}H_3$]coniferyl alcohols (**14**) to *F. intermedia* shoots then established conversion into both secoisolariciresinol (**30**) and matairesinol (**32**) as follows: [8-^{14}C]coniferyl alcohol (**14**) administration revealed that only the (−)-antipodes of secoisolariciresinol (**30b**) and matairesinol (**32b**) were radiolabeled, since the corresponding (+)-antipodes (**30a** and **32a**) were not detectable (see Figure 2 for structures). Additionally, using stable isotopically labeled [9-$^{2}H_2$, OC$^{2}H_3$]coniferyl alcohol (**14**), the (−)-secoisolariciresinol (**30b**) isolated had a m/z 372 (M^+ + 10) indicating that it was derived from intact coupling of two [9-$^{2}H_2$, OC$^{2}H_3$]coniferyl alcohol (**14**) molecules (Davin et al., 1990; Umezawa et al., 1990a, 1991a). In an analogous manner, (−)-octadeuterated matairesinol (**32b**) at m/z 366 (M^+ + 8) was also obtained, suggesting it to be derived directly from [9-$^{2}H_2$,OC$^{2}H_3$]coniferyl alcohol (**14**) as well, presumably via dehydrogenation of (−)-secoisolariciresinol (**30b**). This was confirmed in two ways: administration of (±)-[Ar-^{3}H] and (±)-[Ar-^{2}H]secoisolariciresinols (**30a/b**) individually to *F. intermedia* shoots only gave labeled (−)-matairesinol **32b**, indicative of its formation being a downstream enantiospecific conversion from **30b**. Additional individual experiments using cell-free extracts of *F. intermedia* confirmed further this conversion using (±)-, (+)- and (−)-[Ar-^{3}H]-secoisolariciresinols (**30**) and (±)-[Ar-^{2}H] secoisolariciresinol (**30a/b**), respectively, in the presence of NAD/NADP. Only the (−)-antipode of secoisolariciresinol (**30b**) was converted into (−)-matairesinol (**32b**), whereas the corresponding (+)-enantiomer (**30a**) was not metabolized further.

Lastly, using *F. intermedia* cell-free extracts, it was also demonstrated that coniferyl alcohol (**14**) could be converted into (−)-secoisolariciresinol (**30b**) in the presence of NADPH/H_2O_2, (Davin et al., 1990; Umezawa et al., 1990a, 1991a). When taken together, however, these tracer/stable isotope and cell-free extract data for secoisolariciresinol (**30**) and matairesinol (**32**) biosynthesis only provided a starting point for targeting the proteins and enzymes involved in their biosynthetic pathways. It was unclear at that point as to the number of biosynthetic steps (and proteins or enzymes involved) for each transformation.

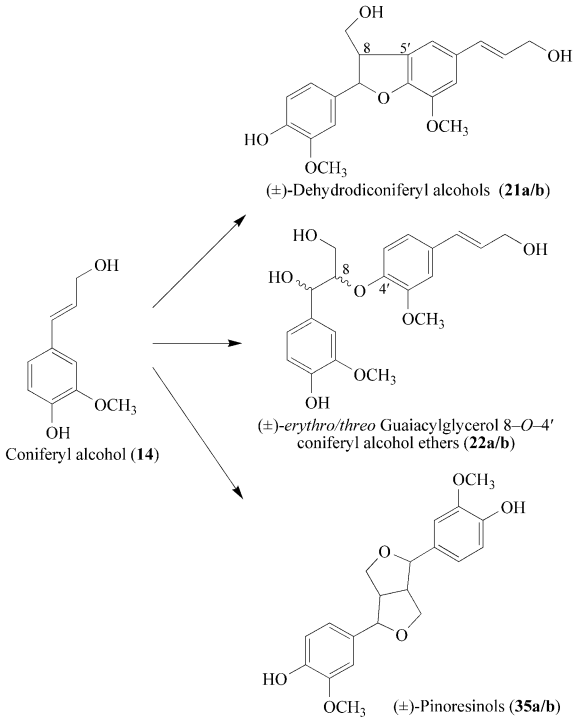

Figure 3. Non-regiospecific ('random') coupling of *E*-coniferyl alcohol (**14**) in presence of one electron oxidase/oxidant and/or H_2O_2/peroxidase.

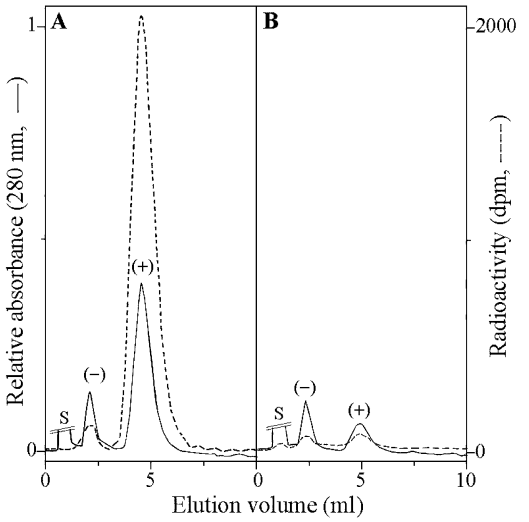

Figure 4. Solubilized proteinaceous mixture capable of catalyzing stereoselective coupling of *E*-[9-^{3}H]coniferyl alcohol (**14**) giving (+)-[9,9′-^{3}H]pinoresinol (**35a**); (**A**) at 21 °C in presence of air and (**B**) at 21 °C under an argon atmosphere. (+) and (−) refer to pinoresinol antipodes (**35a**) and (**35b**), respectively. UV traces show presence of both antipodes due to addition of racemic unlabeled radiochemical carrier (**35a/b**). Redrawn from Paré, Wang, Davin and Lewis (1994). S = solvent.

8–8′ Stereoselective coupling of *E*-coniferyl alcohol: Dirigent protein discovery

With the recognition from the [U-^{14}C]Phe metabolism studies in *F. suspensa* (experimentally carried out by L.B. Davin) that (+)-pinoresinol (**35a**) was the likely initial coupling product in 8–8′ linked lignan biosynthesis, attention was next directed towards defining the biochemical basis for its formation. It was then established that *F. suspensa* stem cell-free extracts were capable of forming the racemic lignans **21a/b**, **22a/b** and **35a/b**, but only when H_2O_2 was added as a co-factor due to non-specific peroxidase-catalyzed coupling (Figure 3). Attention was thus next given to the remaining crude insoluble plant stem material, following removal of readily soluble proteins, this being capable of preferentially converting [8-^{14}C]coniferyl alcohol (**14**) into [8,8′-^{14}C]pinoresinol (**35**), with the (+)-antipode predominating over its (−)-enantiomer in a *circa* 65:35 ratio (Davin et al., 1992). Initial attempts at solubilization of the (+)-pinoresinol-forming system gave extracts able to convert [9-^{3}H]coniferyl alcohol (**14**) into (+)-pinoresinol (**35a**) in a 97% enantiomeric excess (Figure 4A), with all catalytic activity being abolished when air (O_2) was absent (Figure 4B). Confirmation of this transformation was further established using [9-^{2}H$_2$,OC^{2}H$_3$]-coniferyl alcohol (**14**) as substrate (Paré et al., 1994).

Sustained work on isolation of the protein (or proteins) involved in (+)-pinoresinol (**35a**) biosynthesis ultimately afforded a partially purified protein mixture (following several purification steps) which engendered (+)-pinoresinol (**35a**) formation. Subsequent perfusion (POROS-SP-M) chromatography gave a mixture of at least four components (Figure 5A) (Davin et al., 1997), of which Component III (a laccase, Figure 5B) (Lewis et al., 1999) was unexceptionally able to convert [9-^{3}H]coniferyl alcohol (**14**) into the racemic products **21a/b**, **22a/b** and **35a/b** (Figure 3). On the other hand, Component I (Figure 5C) was catalytically inactive; however, when added to the assay solution containing laccase and [9-^{3}H]coniferyl alcohol (**14**), the latter was converted into essentially only (+)-[9,9′-^{3}H]pinoresinol (**35a**). [See time courses of substrate depletion and product formation in the presence and absence of component I, dirigent protein (Figures 6A and 6B).]

This proteinaceous mixture was next demonstrated to only stereoselectively couple coniferyl alcohol (**14**), but not *p*-coumaryl (**38**) or sinapyl (**15**) alcohols

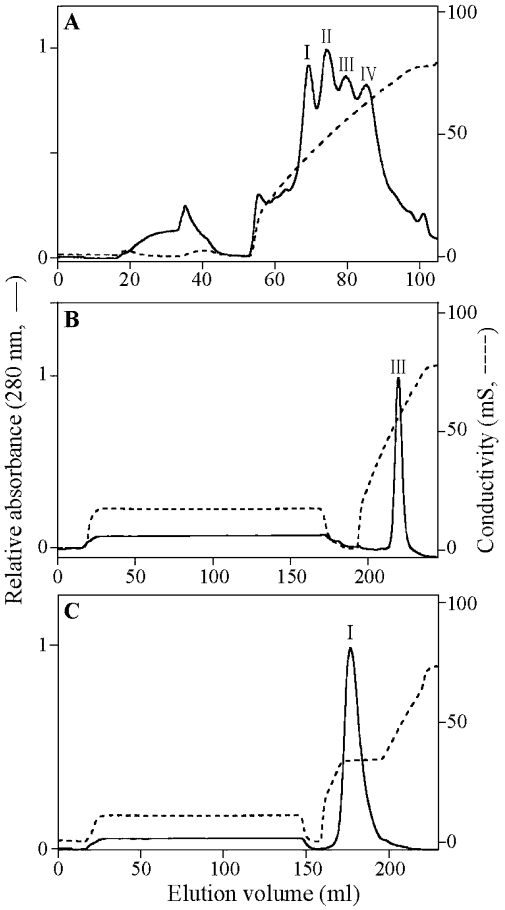

Figure 5. Fractionation of protein mixture catalyzing (+)-pinoresinol (**35a**) formation by perfusion (POROS SP-M) chromatography. (**A**) Separation of proteins into four main overlapping components I–IV, (**B**) Purified component III, (**C**) Purified component I. Redrawn from Davin et al. (1997).

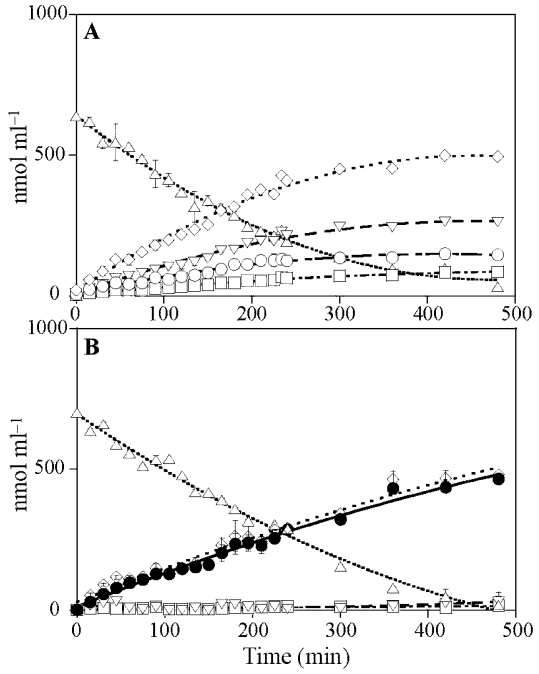

Figure 6. Time courses for *E*-coniferyl alcohol (**14**) depletion and formation of corresponding lignans **21**, **22** and **35** during incubation in presence of: (**A**) component III, laccase (12 μg protein ml^{-1}) and (**B**) component III, laccase (12 μg protein ml^{-1}) and component I (dirigent protein, 770 pmol ml^{-1}). △: coniferyl alcohol (**14**, calculated as dimer equivalents), ●: (+)-pinoresinol (**35a**), ○: (±)-pinoresinols (**35a/b**),: ▽: (±)-dehydrodiconiferyl alcohols (**21a/b**), □: (±)-*erythro/threo* guaiacylglycerol 8–*O*–4′-coniferyl alcohol ethers (**22a/b**), ◇: total of all lignans. Redrawn from Davin et al. (1997).

(which gave racemic products due to non-specific coupling) (Davin et al., 1997). This was an important observation, since it indicated that the dirigent protein binding site(s) was (were) able to distinguish between the three monolignols **14**, **15** and **38**, which differed only in terms of numbers of methoxyl groups. [Interestingly, for (+)-pinoresinol (**35a**) generation, laccase could also be replaced by one-electron oxidants, such as FMN and ammonium peroxydisulfate, i.e. there was no strict requirement for laccase as the one-electron oxidant.] Accordingly, we coined the term dirigent protein for Component I (an ∼26 kDa monomer) from the Latin *dirigere*: to guide or to align (Davin et al., 1997). This terminology was proposed because the protein itself did not apparently affect the rate of one-electron oxidation of coniferyl alcohol (**14**) (i.e. radical generation by the one-electron oxidant/oxidase) but instead appeared to function by binding the free-radical forms so generated, thereby engendering stereoselective rather than racemic coupling. Figure 7 shows the proposed biochemical mechanism for the (+)-pinoresinol forming dirigent protein, where the one-electron oxidant/oxidase generates the free-radical species, which can then bind to generate (+)-pinoresinol (**35a**) via *si-si* coupling as shown.

The corresponding gene encoding the dirigent protein was cloned and found to encode a protein of *circa* 18 kDa, which differed from the native *Forsythia* protein of ∼26 kDa; this difference was due to post-translational glycosylation of the native protein (Gang et al., 1999a). Fully functional (+)-pinoresinol forming dirigent protein (∼26 kDa monomer) was next heterologously expressed using the baculovirus/*Spodoptera* system, although protein expression was generally low (1–2 mg/l) (Gang et al., 1999a). Interestingly, enzymatic deglycosyla-

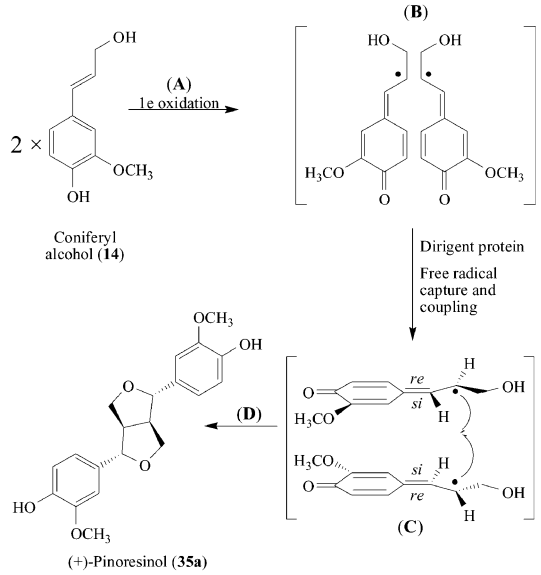

Figure 7. Proposed biochemical mechanism engendered by (+)-pinoresinol forming dirigent protein. (**A**) One electron oxidation to afford free radical form of coniferyl alcohol (**14**), (**B**) capture and alignment of free-radical forms, (**C**) *si-si* coupling and (**D**) intramolecular cyclization of intermediate quinone methide to give (+)-pinoresinol (**35a**).

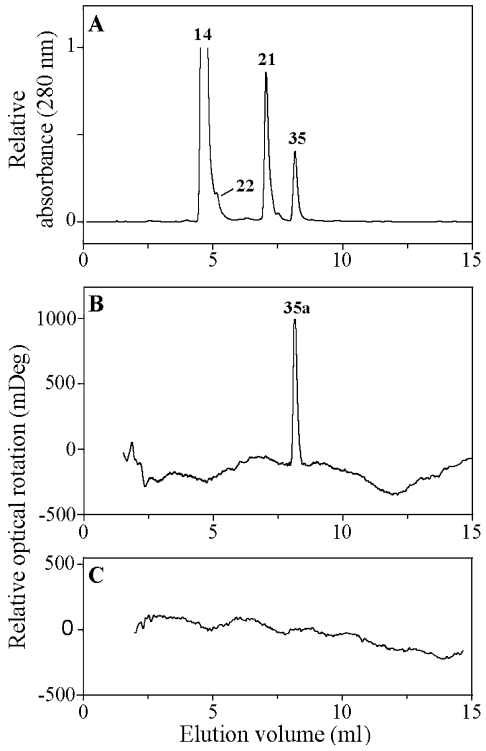

Figure 8. Representative analyses of products from *E*-coniferyl alcohol (**14**) coupling assays, in presence and absence of (+)-pinoresinol forming dirigent protein. (**A**) Reversed-phase C_{18}HPLC separation of complete assay mixture with UV detection, separating monomer **14** from dimers **21**, **22** and **35**; (**B**) laser polarimetric detection, as for A above, revealing presence of (+)-pinoresinol (**35a**) in enantiomeric excess and (**C**) control assay, as for A above, but without dirigent protein. Redrawn from Halls and Lewis (2003).

tion rendered the dirigent protein unable to engender (+)-pinoresinol (**35a**) formation, presumably due to unfolding of the protein.

In order to begin to study the kinetic and biochemical mechanisms associated with the (+)-pinoresinol forming dirigent protein, we developed methodologies to study the stereoselectivity of coupling directly, i.e. without the need for both reversed-phase and chiral HPLC analyses. To do this, a laser polarimeter was placed in-line with the reversed-phase HPLC column with simultaneous UV-detection (Halls and Lewis, 2003). Figure 8A first shows the reversed-phase HPLC chromatogram (UV profile) of a mixture containing coniferyl alcohol (**14**), racemic 8–*O*–4′-linked dimers (**22**) (present as a shoulder under these conditions), racemic 8–5′-linked dehydrodiconiferyl alcohols (**21**) and racemic 8–8′-linked pinoresinols (**35**), generated by non-specific coupling of **14**. In assays containing dirigent protein, however, the (+)-pinoresinol (**35a**) so formed was readily directly detected by laser-polarimetry (Figure 8B), whereas in its absence, only racemic coupling occurred and no measurable optical activity was observed (Figure 8C). [It should also be noted that this method can be used to determine levels of optical purity of known lignans and their derivatives, as well as being amenable for analysis of optically active lignans in crude plant extracts.]

Analysis of the (+)-pinoresinol dirigent protein by sedimentation velocity (ultracentrifugation), MALLS, ESI-MS and MALDI-TOF (Figure 9A) next revealed that the protein existed as a homodimer (with a propensity to aggregate as determined by ultracentrifugation), whereas its CD spectrum established it was composed mainly of β-sheet (9–14%) and loop (40–47%) structures (Figure 9B) (Halls and Lewis, 2002).

It was also of interest to examine some of the basic kinetic parameters, as well as other properties of the native (+)-pinoresinol forming dirigent protein; this included demonstration of its fairly broad pH range (*circa* pH 4–7) and its stability up to about 37 °C (data not shown) (Halls et al., 2004). We also examined substrate binding (equilibrium dialysis) using coniferyl

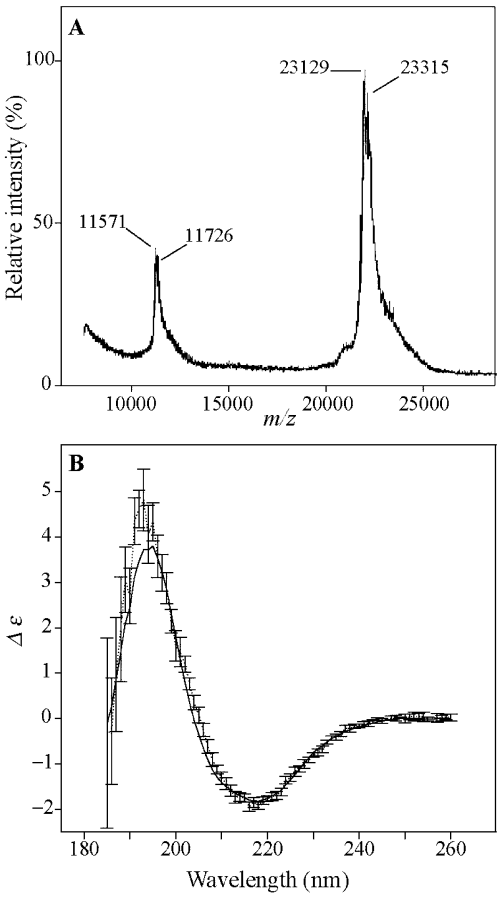

Figure 9. Characterization of (+)-pinoresinol forming dirigent protein. (**A**) MALDI-TOF spectrum, showing both singly and doubly charged monomer masses and (**B**) CD spectrum of *F. intermedia* (+)-pinoresinol forming DP measured at three concentrations and averaged. An expected fit (solid) to the observed CD spectrum (dashed) is shown for a protein with secondary structural components of 40–47% loop, 35–42% β-sheet, 9–14% turn and 5–12% α-helix. Redrawn from Halls and Lewis (2002).

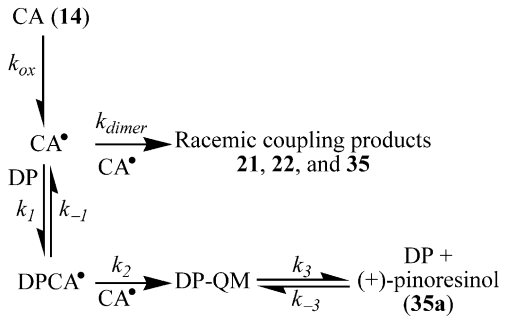

Scheme 3. Proposed kinetic model for stereoselective coupling of coniferyl alcohol radicals in presence of the (+)-pinoresinol forming dirigent protein (DP); non-specific coupling leading to racemic products occurs in absence of the DP. (Redrawn from Halls et al., 2004).

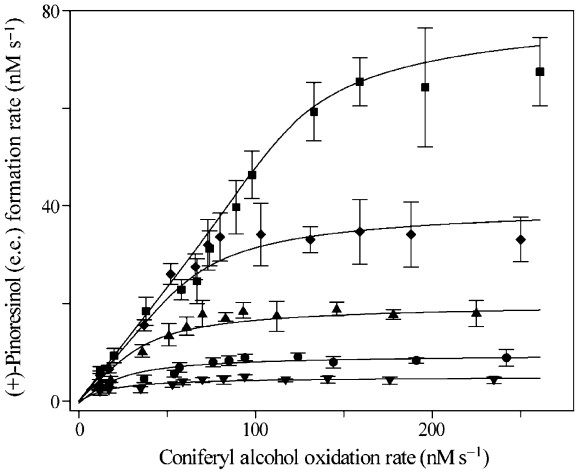

Figure 10. Rate of (+)-pinoresinol (**35a**) production in enantiomeric excess, as a function of different coniferyl alcohol (**14**) oxidation rates and in the presence of different DP dimer concentrations: (▼) 20 nM, (●) 40 nM, (▲) 80 nM, (♦) 160 nM and (■) 320 nM, respectively. [e.e.: enantiomeric excess.] Redrawn from Halls et al. (2004).

(**14**), sinapyl (**15**) and *p*-coumaryl (**38**) alcohols, respectively. However, the data obtained revealed that extremely weak binding of only coniferyl alcohol (**14**) occurred, with a K_D of 370 ± 65 μM, and thus was the unlikely proper substrate for the dirigent protein (i.e., the presumed correct substrate being the free-radical form of **14**); there was no evidence for even weak binding of the other two monolignols **15** and **38**. On the other hand, it was observed that two coniferyl alcohol (**14**) molecules were weakly bound per homodimer, suggesting the presence of one substrate binding site per protein monomer (Halls et al., 2004).

Several kinetic models for the (+)-pinoresinol forming dirigent protein were next considered, with an iterative algorithm giving one mechanistic model as being the most likely (Scheme 3). That is, following oxidation of coniferyl alcohol (**14**) to its free radical form CA• *in vitro*, competition between two processes can result. The first is that occurring in open solution and leading to racemic products **21**, **22** and **35**, whereas the second is that of two CA• molecules sequentially binding to the dirigent protein in a cooperative, anti-cooperative or independent manner to give (+)-pinoresinol (**35a**). In this regard, Figure 10 summarizes the effects observed of varying both the coniferyl alcohol (**14**) oxidation rate and dirigent protein concentration on (+)-pinoresinol (**35a**) generation in enantiomeric excess. Note that at each concen-

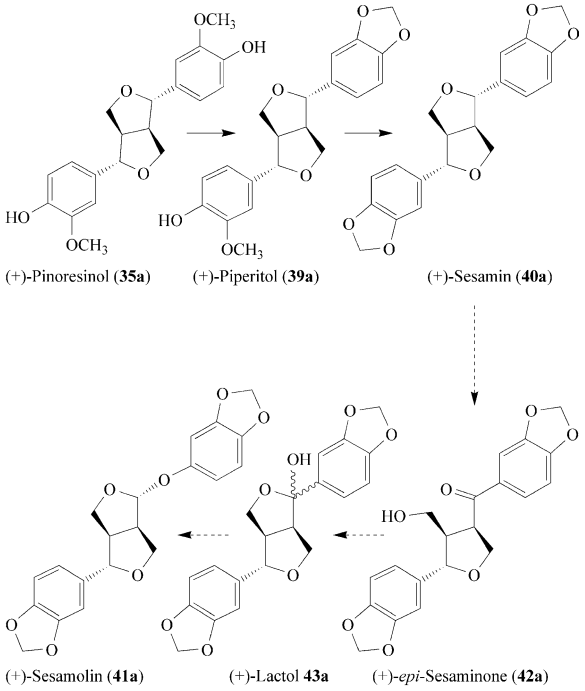

Figure 11. Possible biochemical pathway to (+)-sesamolin (**41a**) from (+)-pinoresinol (**35a**).

tration examined (20–320 μM), the dirigent protein can be saturated, with the 320 μM concentration representing the upper limit of dirigent protein needed to successfully outcompete all non-specific coupling (i.e., relative to the free radical generation/coniferyl alcohol (**14**) oxidation rate being used). Scheme 3 is thus in agreement with the observed data, with K_1 estimated to be 10 nM with a $k_1 \sim 1.7 \times 10^8$ s^{-1} for binding of the CA$^\bullet$ to the unoccupied complex, whereas binding of the second CA$^\bullet$ (essentially irreversible) to give the intermediate quinone methide (DP-QM) was estimated as $k_2 \sim 2.1 \times 10^8$ s^{-1}. Additionally, estimates of the coupling rate constants for release of product, (+)-pinoresinol **35a**, were slow with $k_3 \sim 0.27$ s^{-1} ($K_3 \sim 1.9$) in harmony with the measured $k_{fwd} \sim 0.26 \pm 0.3$ s^{-1} (see Halls et al., 2004, for additional details in developing this model). Taken together, all available data are consistent with the dirigent protein (sequentially) binding free-radical forms of coniferyl alcohol (**14**), and processing same to afford (+)-pinoresinol (**35a**).

Dirigent proteins and downstream metabolism in sesame seeds

Sesame (*Sesamum indicum*) seeds accumulate various antioxidant lignans, such as (+)-piperitol (**39a**), (+)-sesamin (**40a**) and (+)-sesamolin (**41a**) (Figure 11). All possess pinoresinol-like features, but differ through either methylenedioxy bridge formation, oxygen insertion between the furan and aromatic rings, or both. It was, therefore, of interest to investigate the biochemical pathways in this species and whether dirigent-protein mediated transformations were also operative. Thus, radiolabeling experiments, using intact *S. indicum* seeds, next revealed that [8-^{14}C]coniferyl alcohol (**14**) was indeed metabolized into (+)-pinoresinol (**35a**), and additional studies using (+)- and (−)-[3,3′-O^{14}CH$_3$]pinoresinols (**35a/b**) and (±)-[3-O^{14}CH$_3$]piperitols (**39a/b**) established that only the (+)-antipodes of each were converted into (+)-piperitol (**39a**), (+)-sesamin (**40a**) and (+)-sesamolin (**41a**), respectively. The corresponding (−)-enantiomers were not utilized, in agreement with earlier observations on *E*-coniferyl alcohol (**14**) metabolism in this species (Jiao et al., 1998; Kato et al., 1998). Moreover, methylenedioxy bridge formation from (+)-pinoresinol (**35a**) to both piperitol (**39a**) and (+)-sesamin (**40a**) was established to be cytochrome P-450 and NADPH-dependent (Jiao et al., 1998), whereas the oxygen insertion step was provisionally concluded to involve (+)-*epi*-sesaminone (**42a**) as an intermediate (Figure 11). The latter is possibly derived from (+)-sesamin (**40a**) via a single hydroxylation step. This, via the lactol form (+)-*epi*-sesaminone (**43a**), may in turn undergo enzyme-modulated rearrangement to introduce the oxygen functionality between the aromatic and furano ring systems (Marchand et al., 1997a,b). However, to this point, this latter transformation has not been investigated at the enzyme level.

Dirigent protein and dirigent sites: Ramifications for lignan and lignin biosynthesis

Tissue specific expression of the dirigent protein gene was next examined in various *F. intermedia* organs using a combination of *in situ* mRNA hybridization and immunolocalization techniques (Burlat et al., 2001; Kwon et al., 1999). Dirigent protein mRNA localization was first studied by tissue printing hybridization of fresh cross-sections of *F. intermedia* stems, petioles and roots. This revealed the presence of intense

signals in all tissues examined (as compared to the corresponding controls). In the stem cross-sections, the signal was associated with the cambial regions in all developmental stages investigated (i.e. from the 1st, 10th and 20th internodes). At earlier stages of development, the signal was also present in the cortex and the pith but the intensity of labeling decreased with stem maturation. In both petioles and roots, the signal was also associated with the cambial regions (Burlat et al., 2001; Kwon et al., 1999). These observations were further confirmed by *in situ* hybridization of the dirigent protein mRNA using digoxigenin labeled riboprobes in stem cross-sections (Burlat et al., 2001; Davin and Lewis, 2000; Kwon et al., 1999). At this level of resolution, it was possible to demonstrate that dirigent protein expression was associated not only with the cambial regions in the youngest development stage studied (1st internode) but also with ray parenchyma initials adjacent to lignified tracheary elements which only displayed a weak signal.

The dirigent protein and presumed homologs harboring dirigent sites (monolignol radical binding sites) were next localized at the tissue and subcellular levels using polyclonal antibodies raised against the dirigent protein (Burlat et al., 2001; Davin and Lewis, 2000). Polyclonal antibodies were employed in order to assess if dirigent sites (dirigent homologs or related proteins containing an array of dirigent sites) were involved in lignification as well as in lignan biosynthesis. Thus, using thick sections of paraffin embedded samples, the antibody response was localized in both the vascular cambium region and young developing xylem, together with labeling in the cortex outer layers. With stem maturation, however, the signal became restricted to the vascular cambium region (cambium and secondary phloem), and to lignified cells of secondary xylem, sclerified pith parenchyma, and phloem fibers. In mature petioles, the labeling was also mainly restricted to the cambial layers, the secondary phloem and the developing xylem, whereas in the roots labeling was in the pericycle layers together with the vascular tissues of the stele. These patterns of dirigent protein localization were thus similar to those observed for dirigent gene expression, with the only difference being that the antibodies also revealed cross-reactivity within lignified elements.

Immunolabeling experiments were next conducted on resin embedded samples, with high resolution transmission electron microscopy being employed in order to localize dirigent protein/dirigent sites at the subcellular level (Burlat et al., 2001; Davin and Lewis, 2000). It was found that labeling was predominantly in the S1 sub-layer and compound middle lamella, i.e. in regions where lignification is initiated, and to a lesser extent in the fully developed S3 layer of fully developed vessels and developing ray cells (Burlat et al., 2001). In lignified phloem, however, labeling was associated with the S1 sub-layer in both young and mature fibers, whereas in the metaxylem secondary wall cross-reactivity was distributed throughout the wall, which has an uniform thickening. Taken together, these data suggested that there were two populations of dirigent protein/proteins harboring (arrays of) dirigent sites, i.e. cambial/ray parenchyma initials which were involved in lignan biosynthesis, and precise areas with the secondary wall involved in lignin formation.

Pinoresinol-lariciresinol reductases: Enzyme mechanism and molecular basis for differing enantiospecificities

Our earlier preliminary work (described above) using *F. intermedia* cell-free extracts had indicated that coniferyl alcohol (**14**) could be converted into (−)-secoisolariciresinol (**30b**), in the presence of NADPH/H_2O_2 (Umezawa et al., 1990a,b, 1991a). However, since related studies with *F. suspensa* (Davin et al., 1992) had also demonstrated compelling evidence for stereoselective coupling of *E*-coniferyl alcohol (**14**) giving (+)-pinoresinol (**35a**), attention was given to the actual underlying biochemical processes accounting for (−)-secoisolariciresinol (**30b**) formation in *F. intermedia*, and whether this occurred via the intermediacy of (+)-pinoresinol (**35a**).

We thus next demonstrated that the *F. intermedia* cell-free extracts, when incubated with [8-^{14}C]coniferyl alcohol (**14**) in the presence of exogenously added H_2O_2, actually generated (±)-racemic pinoresinols (**35a/b**) in addition to the other non-specific coupling products **21a/b** and **22a/b**, due to the action of non-specific peroxidases. However, when NADPH was also present, the (+)-antipode of racemic (±)-[8,8′-^{14}C]pinoresinols (**35a/b**) was selectively metabolized ultimately affording (−)-[8,8′-^{14}C]secoisolariciresinol (**30b**); by contrast, the (−)-antipode (**35b**) was not metabolized further (Katayama et al., 1992). [Note also, however, that stereoselective coupling of coniferyl alcohol (**14**) to give (+)-pinoresinol (**35a**) occurred with the *F. intermedia* insoluble residue, i.e. the generation of racemic pinoresinols (**35a/b**) was an artifact produced

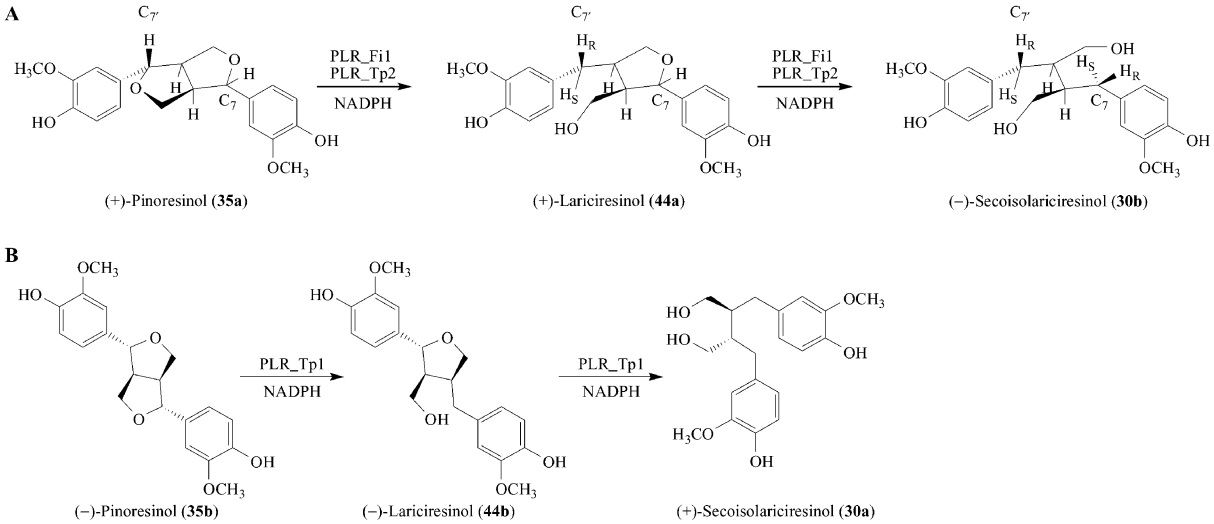

Figure 12. Enantiospecific reactions catalyzed by *F. intermedia* and *T. plicata* pinoresinol/lariciresinol reductases (PLR). (**A**) PLR_Fi1 and PLR_Tp2 catalyzing the conversion of (+)-pinoresinol (**35a**) into (−)-secoisolariciresinol (**30b**), (**B**) PLR_Tp1 catalyzing opposite enantiospecific conversion. PLR_Fi1: *F. intermedia*1; PLR_Tp1: *T. plicata* 1; PLR_Tp2: *T. plicata* 2.

by the soluble crude extract mixture.] Additionally, when the (+)- and (−)-enantiomers of pinoresinol (**35a**) and (**35b**) were individually incubated with the *F. intermedia* cell-free extracts, in the presence of NADPH, preferential conversion was observed into both (+)-lariciresinol (**44a**) [i.e., 99:1 in favor of the (+)-antipode (**44a**) over the (−) enantiomer (**44b**)] and (−)-secoisolariciresinol (**30b**), respectively (Figure 12A). Incubation with (±)-lariciresinols (**44a/b**) also established that only the (+)-antipode (**44a**) was converted into (−)-secoisolariciresinol (**30b**) (Katayama et al., 1993). Taken together, these data revealed the existence of a bifunctional enantiospecific pinoresinol-lariciresinol reductase in the readily soluble protein extract of *F. intermedia* which utilized both (+)-pinoresinol (**35a**) and (+)-lariciresinol (**44a**). These data thus eliminated the possibility that (−)-secoisolariciresinol (**30b**) was being formed directly from coniferyl alcohol (**14**) in the presence of H_2O_2/NADPH and the *F. intermedia* cell-free extracts.

The reductive conversion of (+)-pinoresinol (**35a**) into (+)-lariciresinol (**44a**) and (−)-secoisolariciresinol (**30b**) was also demonstrated to occur via abstraction of the 4-pro-R hydrogen from NADPH (using either specifically labeled 4*R*- and 4*S*-^{3}H/^{2}H-NADPH) (Chu et al., 1993; Dinkova-Kostova et al., 1996), i.e., in a manner analogous to that of cinnamyl alcohol dehydrogenase (Mansell et al., 1974). Additionally, using synthetic [7,7′-$^2H_2$]pinoresinol (**35**) and [7,7′-$^2H_3$]lariciresinol (**44**) as substrates, it was established that the incoming hydride (from unlabeled NADPH) took up the pro-*R* position at C-7′ in lariciresinol (**44**) and at C-7/C-7′ in secoisolariciresinol (**30**), respectively, i.e., the reductase steps were highly stereospecific (>99%) (Chu et al., 1993).

This is schematically shown in Figure 12A, where the incoming hydride [which ultimately reduces the furanofuran rings] takes up the pro-*R* positions at C-7/C-7′, the overall effect of which is an inversion of configuration at these positions. This was evidenced by ^{1}H-NMR spectral analysis of the enzymatic products, (+)-[7,7′ *S*-$^2H_2$]lariciresinol (**44a**) and (−)-[7,7′ *S*-$^2H_3$]secoisolariciresinol (**30b**), formed following incubation of [7,7′-$^2H_3$]pinoresinol (**35**) and [7,7′-$^2H_3$]lariciresinol (**44**), respectively, with the partially purified PLR (Chu et al., 1993). For example, Figure 13A shows the partial ^{1}H-NMR spectrum of synthetic (±)-lariciresinols (**44a/b**), whereby the $C_{7'}$HS, $C_{8'}$H, $C_{7'}$H*R* and C_8H protons are readily distinguishable, in contrast to that of enzymatically synthesized (+)-[7,7′ *S*-$^2H_2$]lariciresinol (**44a**) (Figure 13B) where the $C_{7'}$H*S* proton is not detectable (being deuterated) with concomitant simplification of coupling at $C_{7'}$H*R*. This, therefore, established that inversion of configuration at C-7/C-7′ upon enzymatic reduction had occurred (Chu et al., 1993).

That the protein was in fact a bifunctional pinoresinol-lariciresinol reductase (PLR) was unambiguously demonstrated by purification (∼3,000-fold) of two *F. intermedia* PLR isoforms to apparent ho-

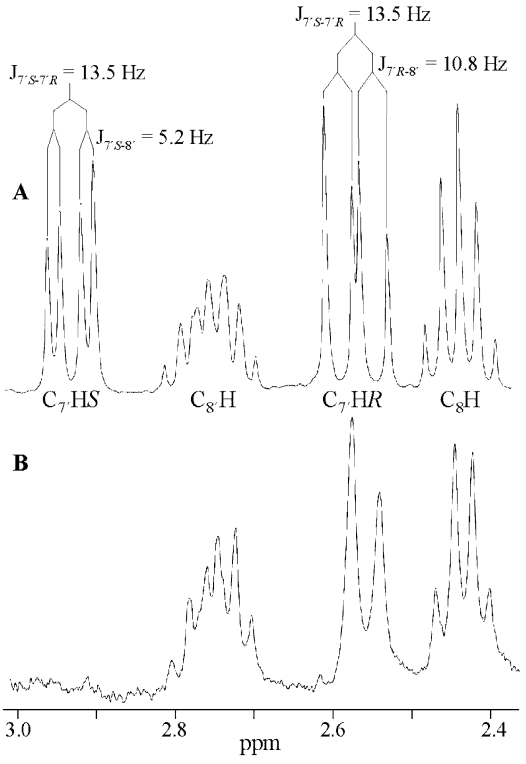

Figure 13. Partial ^{1}H NMR spectra of lariciresinol (**44**) showing spectral regions for C-7′, C-8′ and C-8 proton resonances. (**A**) Synthetic (±)-lariciresinols (**44a/b**), and (**B**) enzymatically synthesized (+)-[7,7′ *S*-$^{2}H_2$]lariciresinol (**44a**). Redrawn from Chu et al. (1993).

mogeneity, with each (~34.9 kDa monomer) being subjected to detailed kinetic analysis and giving essentially the same catalytic properties, i.e., K_m for (+)-pinoresinol (**35a**), 27 ± 1.5 and 23 ± 1.3 μM; K_m for (+)-lariciresinol (**44a**) 121 ± 5.0 and 123 ± 6.0 μM; V_{max} (+)-pinoresinol (**35a**), 16.2 ± 0.4 and 17.3 ± 0.5 μmol h^{-1} mg^{-1} protein and for (+)-lariciresinol (**44a**), 25.2 ± 0.7 and 29.9 ± 0.7 μmol h^{-1} mg^{-1} protein, respectively (Dinkova-Kostova et al., 1996).

The corresponding encoding gene was cloned (e.g., PLR_Fi1), with heterologous expression of fully functional catalytic PLR being initially obtained as its β-galactosidase fusion adduct (Dinkova-Kostova et al., 1996). Interestingly, in western red cedar (*T. plicata*), which accumulates various 8–8′ linked lignans, such as plicatic acid (**20**) (Figure 14), two forms of PLR were found to be present (Fujita et al., 1999). Each was expressed heterologously as a β-galactosidase fusion adduct in *E. coli*, and each displayed distinct enantiospecificities, i.e., PLR_Tp2 was capable of enantiospecifically converting (+)-pinoresinol (**35a**) into (+)-lariciresinol (**44a**) and (−)-secoisolariciresinol (**30b**), whereas PLR_Tp1 catalyzed the opposite conversions (Figures 12A and 12B) (Fujita et al., 1999).

PLR_Tp1 has since been crystallized and its crystal structure solved (to 2.5 Å) which, when modeled with PLR_Tp2, provides an explanation for the differing enantiospecificities (Min et al., 2003). Both structures have a continuous alpha/beta NADPH binding domain and a smaller substrate-binding domain. The schematic representations of PLR_Tp1 and the energy minimized model of PLR_Tp2 are depicted in Figures 15A and 15B, respectively, with both having completely conserved 'GXXGXXG' NAD(P)H binding motif sequences at the first β-α-β unit. Interestingly, a BLAST search of the Protein Data Bank revealed that PLR had a good level of similarity to that of *E. coli* UDP-galactose epimerase. Hence, by comparison of the three-dimensional topology and amino acid sequences of UDP-galactose 4-epimerase C-terminal domains with those of PLR_Tp1 (and, by analogy, PLR_Tp2), it was possible to identify putative substrate binding pockets. These are made up of two β-strands (in a small 3-stranded, antiparallel β-sheet) and two α-helical segments, and are mostly hydrophobic in character. The substrate binding sites are adjacent to the cofactor, so that the substrate molecules [(−)- and (+)-pinoresinols (**35b** and **35a**), (−)- and (+)-lariciresinols (**44b** and **44a**), respectively] are neatly juxtaposed for direct 4*R*-hydride transfer from the NADPH cofactor. Based on such comparative analyses, it was also deduced that PLR_Tp1 and related homologs (Min et al., 2003) all contained a conserved Lys residue (Lys^{138} in PLR_Tp1) required for general base catalysis. Indeed, site-directed mutagenesis (Lys^{138} → Ala^{138}) resulted in abolition of enzymatic activity of PLR_Tp1. Differences in enantiospecificity of both PLR_Tp1 and PLR_Tp2 could also be rationalized, since (−)-pinoresinol (**35b**) fits snugly among the hydrophobic side-chains of Phe^{164}, Val^{268} and Leu^{272}, whereas in PLR_Tp2 binding of the (+)-antipode of pinoresinol (**35a**) is favored by a symmetric substitution of residues at 164 and 272 (i.e., Leu^{164} and Phe^{272}), as well as the residue at 268 becoming glycine.

In situ hybridization of PLR was also carried out with *F. intermedia* stems at different stages of development (i.e., 1st, 2nd, 10th and 20th internodes) as well as roots, petioles and leaves, with serial sections prepared from paraffin-embedded tissues (Kwon et al., 2001). The strongest signal was found in the stems

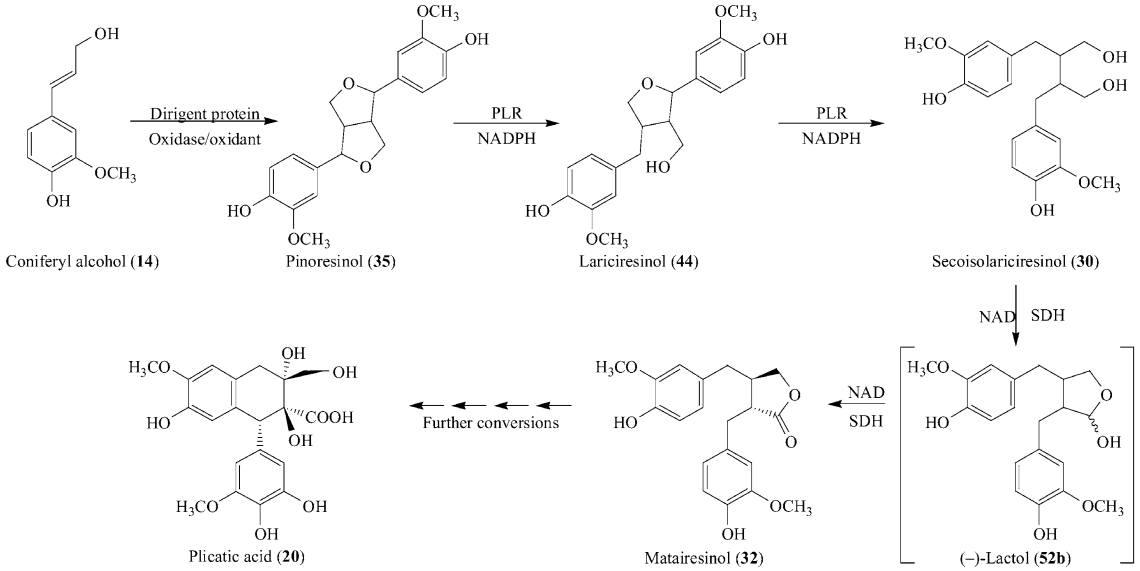

Figure 14. Biosynthetic pathway to matairesinol in *F. intermedia/P. peltatum* and proposed biosynthetic pathway to plicatic acid (**20**), a major constituent of western red cedar (*T. plicata*) heartwood.

as compared to the roots, petioles and leaves. In stem sections, PLR mRNA accumulation was mainly associated with the vascular cambium and differentiating xylem, with levels of detectable mRNA decreasing with stem maturation (i.e., from the 1st to the 20th internode). A faint signal was also noted in the cortex at early stages of development (1st and 2nd internodes). In the roots, petioles and leaves, mRNA accumulation was localized within the meristematic tissues (Kwon et al., 2001).

Biosynthetic pathways to secoisolariciresinol diglucoside-hydroxymethyl glutaryl ester linked lignan oligomers in flax seed (Linum usitatissimum)

Recent studies in our laboratory established that flaxseed contains various ester-linked oligomers of secoisolariciresinol diglucoside (SDG, **31**) covalently linked to hydroxymethyl glutaryl moieties (HMG, **45**), e.g., **46–49** (Scheme 4) (Ford et al., 2001). Related compounds have also been reported by Kamal-Eldin et al. (2001). Interestingly, flaxseed has long been known to be a source of SDG (**31**) (Bakke and Klosterman, 1956), and this compound is believed to be a cancer chemopreventative agent effective against the onset of breast, prostrate and colon cancers (Jenab and Thompson, 1996; Thompson et al., 1996a,b). SDG (**31**) (and matairesinol (**32**) in other species) are metabolized by (anaerobic) intestinal bacteria (Borriello et al., 1985) to generate both enterodiol (**50**) and enterolactone (**51**), with the proposed pathways to these being summarized elsewhere (Ford et al., 1999; Teoh et al., 2003). In terms of their physiological roles, enterodiol (**50**) and enterolactone (**51**), are thought to be able to modulate various aspects of sex hormone metabolism (Martin et al., 1996; Mousavi and Adlercreutz, 1992), as well as inhibiting cell proliferation and angiogenesis (Thompson et al., 1996a,b). SDG (**31**) (and flax seed) can also reduce plasma insulin growth factor 1 in rats, this being correlated with a decreased breast cancer risk (Rickard et al., 2000).

Our current interests have been in studying the biochemical pathway to both SDG (**31**) and its various oligomers (e.g., **46–49**) in developing flaxseed, using tracer/stable isotope studies and molecular approaches to identify both intermediates and genes/proteins/enzymes involved. Interestingly, at all stages of flax seed development, essentially no SDG (**31**) is present in its free form, but is instead covalently linked (via ester-linkages) to other constituents, e.g. **45** and **46**; SDG (**31**) can, however, be readily released upon mild alkaline hydrolysis at ambient temperature (Ford et al., 2001). Interestingly, there are two distinct diastereomers of SDG (**31**) present in flaxseed; the dominant form (∼99%) is (+)-secoisolariciresinol (**30a**) and the minor (∼1%), the opposite antipode (**30b**) (Ford et al., 2001). Recognition of this raised the possibility of two distinct biochemical pathways to each of the (+)- and (−)-secoisolariciresinol

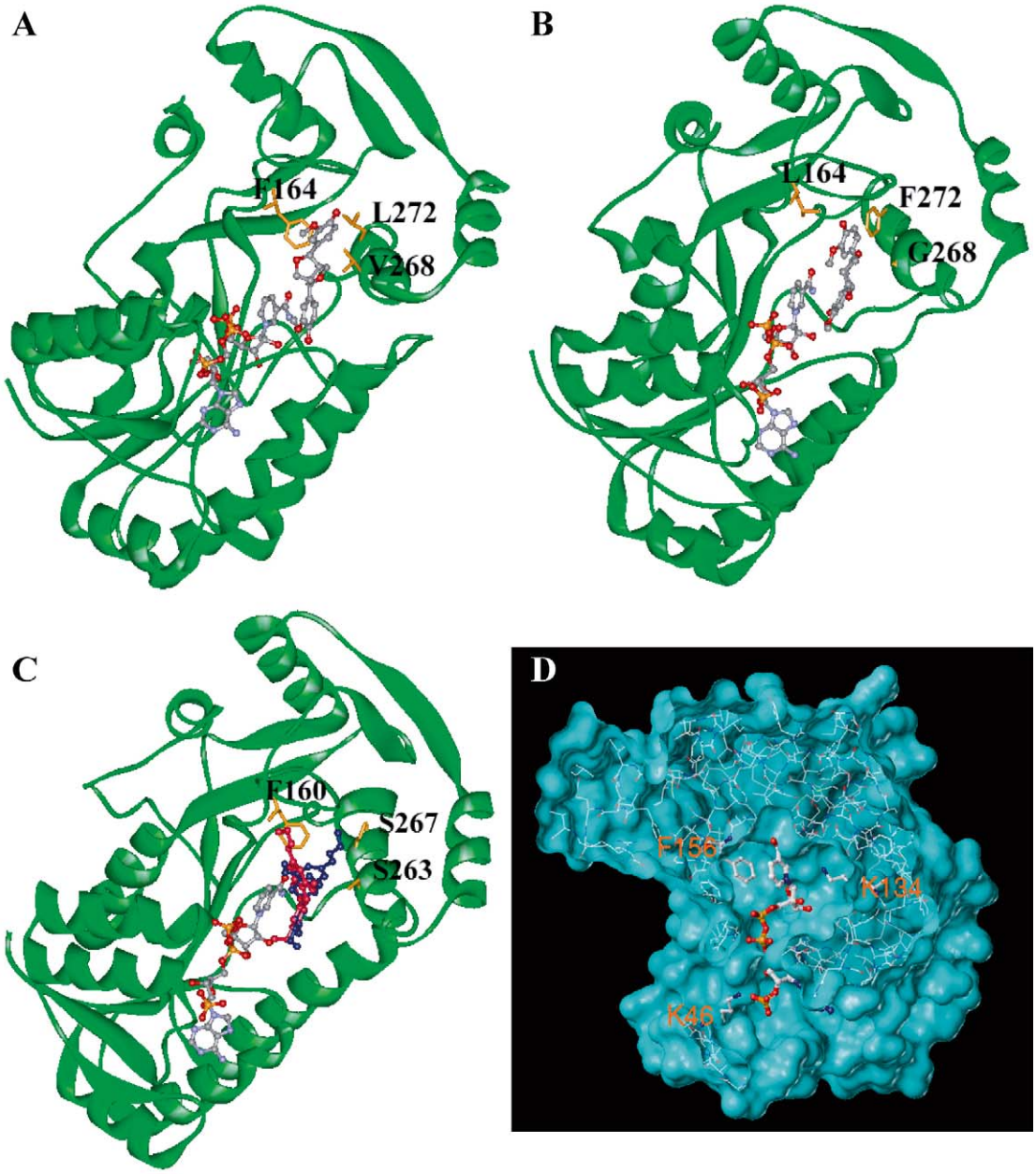

Figure 15. X-ray crystal structures of PLR and PCBER and molecular surface of PCBER. Schematic representation of the crystal structures of PLR_Tp1 (**A**) and PCBER_Pt1 (**C**), and the energy minimized models of PLR_Tp2 (**B**), together with NADPH and the corresponding lignan substrates. The potential key residues that form substrate contact points and possibly cause unique specificities are highlighted. [In (**C**), the (+)- and (−)-forms of dehydrodiconiferyl alcohol (**21**) are depicted in blue and red, respectively]. Molecular surface of PCBER-Pt1 showing the NADPH binding pocket (**D**): the side-chain of Phe^{156} is in a stacking mode with the nicotine amide ring, and the side-chain of Lys^{46} is salt-bridged with the 2′-phosphate group of the NADPH. The putative catalytic residue Lys^{134} in PCBER (Lys^{138} in PLR) can serve as a general base. Redrawn from Min et al. (2003).

(**30a/30b**) forms. Thus, a significant effort was applied to the study of SDG (**31**) formation, this involving both detection of a (−)-pinoresinol (**35b**) forming system (unpublished data), together with heterologous expression (*Drosophila* system) of a flaxseed protein encoded by a dirigent gene homolog; this recombinant flaxseed dirigent protein, however, engendered only (+)-pinoresinol (**35a**) formation, in agreement with

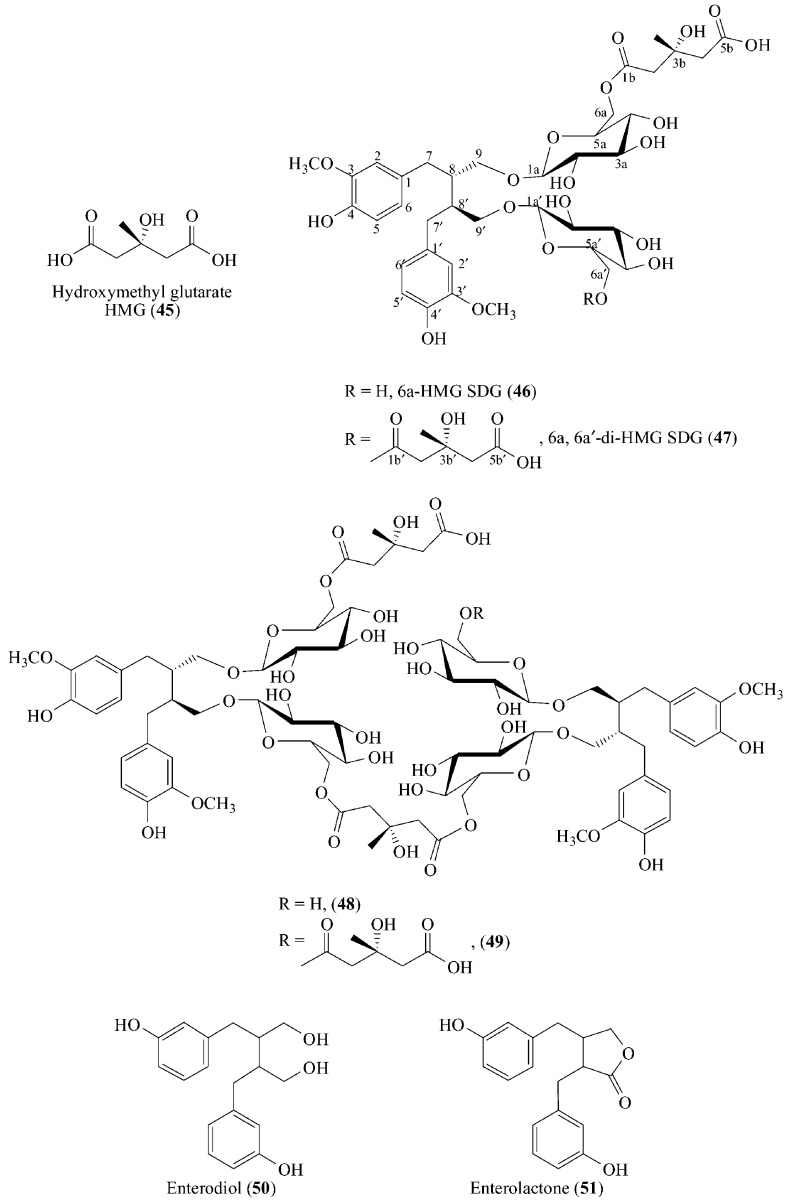

Scheme 4. HMG (**45**), and SDG-HMG oligomeric constituents (**46**–**49**) of flaxseed, together with 'mammalian' lignans, enterodiol (**50**) and enterolactone (**51**).

there being two pathways to SDG (**31**), i.e. the major involving (+)-secoisolariciresinol (**30a**) formation and the minor to (−)-secoisolariciresinol (**30b**). Additionally, it was found that when a 40–80% $(NH_4)_2SO_4$ protein fraction from flaxseed was incubated with (±)-[3,3′-O^{14}CH$_3$]-pinoresinol (**35a/b**) and NADPH at 32 °C for 12 h, both (+)-[3,3′-O^{14}CH$_3$] lariciresinol (**44a**) and (+)-[3,3′-O^{14}CH$_3$]-secoisolariciresinol (**30a**) were formed. A PLR cDNA (*PLR_Lu*) was also isolated from a flaxseed cDNA library, which displayed 68% similarity and 58% identity to PLR_Tp1. Heterologous expression of *PLR_Lu* in *E. coli* was next carried out and it was shown that formation of (−)-lariciresinol (**44b**) was obtained when PLR_Lu was incubated with (−)-pinoresinol (**35b**) in presence of [4*R*-^{3}H] NADPH; no conversion was observed when either (+)- or (±)-pinoresinols (**35a** and **35a/b**) were used as substrates, perhaps indicative of inhibition by the (+)-antipode (**35a**) (Teoh et al., manuscript in preparation). These results thus seem to support the

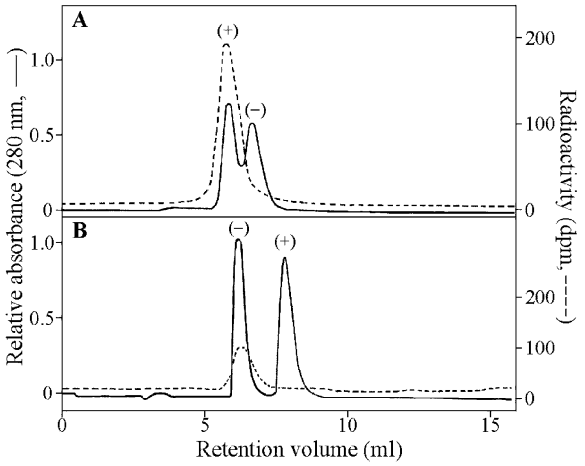

Figure 16. Chiral column HPLC analysis of lignan products obtained following enzymatic reduction of (±)-pinoresinols (**35a/b**) with *L. flavum* root cell-free extracts, in the presence of [4*R*-^{3}H]NADPH. (**A**) [7-^{3}H]lariciresinol (**44**) and (**B**) [7,7′-^{3}H]secoisolariciresinol (**30**). [Note: Unlabeled radiochemical carriers of racemic (±) **44a/b** and (±) **30a/b** were added following assay termination. (−) and (+) refer to antipodes of **44** (**A**) and **30** (**B**), respectively. Redrawn from Xia et al. (2000).

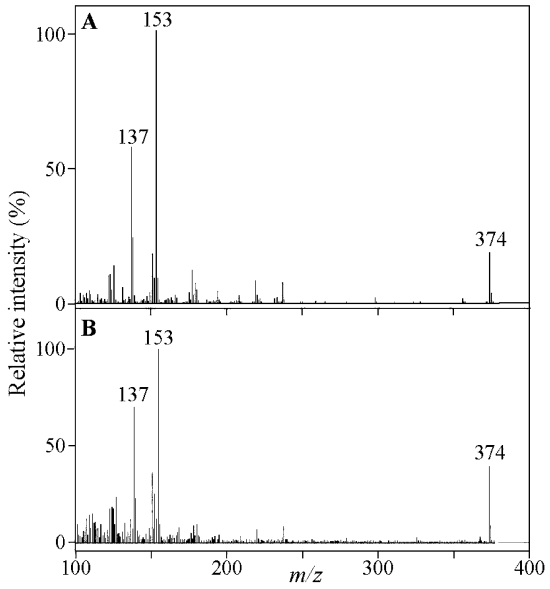

Figure 17. Mass spectral fragmentation pattern (EI mode) of (**A**) synthetic 7′-hydroxymatairesinol (**54**), and (**B**) 7′-hydroxymatairesinol (**54**) obtained after administration of matairesinol (**32**) to *L. flavum* root tissue. Redrawn from Xia et al. (2000).

presence of 2 independent pathways to both (+)- and (−)-secoisolariciresinol (**30a** and **30b**) as proposed in western red cedar.

Secoisolariciresinol dehydrogenase (SDH)

As described above, preliminary radiotracer/stable isotope studies using both *F. intermedia* whole plants, and cell-free extracts therefrom, indicated that (−)-secoisolariciresinol (**30b**) could be converted into (−)-matairesinol (**32b**) (Umezawa et al., 1991a), whereas the (+)-enantiomer (**30a**) was not metabolized further. However, it was unknown at that time whether this NAD-dependent enantiospecific conversion involved either a bifunctional secoisolariciresinol dehydrogenase (SDH) with intermediacy of lactol (**52**), or whether two enzymes were required, i.e., one to form (−)-lactol (**52b**) and the other to convert it into (−)-matairesinol (**32b**) (Figure 14).

This particular question was resolved in two ways (Xia et al., 2001): first, by purifying (>6,000-fold) an ∼32 kDa protein from *F. intermedia* capable of converting (−)-secoisolariciresinol (**30b**) into (−)-matairesinol (**32b**), and secondly, by cloning the encoding gene and establishing that the heterologously expressed recombinant SDH (in *E. coli*) was able to enantiospecifically convert (−)-secoisolariciresinol (**30b**) into (−)-matairesinol (**32b**) (Xia et al., 2001). Interestingly, with recombinant protein assays using (−)-secoisolariciresinol (**30b**) in the presence of NAD, (−)-lactol (**52b**) was isolated as an intermediate as well as the end-product, (−)-matairesinol (**32b**). Thus, (−)-matairesinol (**32b**) formation utilized an enantiospecific bifunctional NAD-dependent reductase and not two distinct enzymes. With the gene encoding SDH in hand, the entire biochemical pathway from *E*-coniferyl alcohol (**14**) to matairesinol (**32**) was fully elucidated at both enzyme and gene levels (Xia et al., 2001).

Related studies by others on lariciresinol, secoisolariciresinol and matairesinol formation

Since leaving the Lewis group as a postdoctoral associate, Umezawa and coworkers have subsequently carried out a number of closely related studies with crude cell-free extracts of various plant species. For example, in the presence of NADPH/H_2O_2, they subsequently demonstrated that crude cell-free extracts of *Forsythia koreana* were able to convert coniferyl alcohol (**14**) into (−)-secoisolariciresinol (**30b**) (Umezawa

et al., 1992, 1994), thus providing further confirmation of our original findings. The same investigators also examined cell-free extracts of *Arctium lappa* ripening seeds, which in the presence of NADPH/H_2O_2, gave mixtures consisting of (−)-pinoresinol (**35b**, 22% enantiomeric excess, e.e.), (−)-lariciresinol (**44b,** >99% e.e.) and (−)-secoisolariciresinol (**30b**, 38% e.e.) (Susuki et al., 1998, 1999, 2002b), respectively, but again with no clarification of either the stereoselectivity or enantiospecificity of any of the proteins or enzymes actually involved. Additionally, when cell free extracts of *A. lappa* petioles were incubated in the presence of coniferyl alcohol (**14**)/NADPH/H_2O_2 as before, the assay mixture contained (+)-pinoresinol (**35a**) in 33% e.e., as well as (+)-lariciresinol (**44a**) in 30% e.e. and (+)-secoisolariciresinol (**30a**) in 20% e.e. (Susuki et al., 2002b; Umezawa and Shimada, 1996). These results, using crude protein extracts, seem to be in agreement with a dual pathway (in petioles and ripening seeds) leading to both (+) and (−)-secoisolariciresinols (**30a** and **30b**), i.e. as previously definitively demonstrated by our laboratory with western red cedar (Fujita et al., 1999). However, again, since there was no isolation and characterization of any of the proteins/enzymes involved, no definitive clarification of the stereoselectivity and enantiospecificity of these transformations was achieved.

However, these studies by Umezawa et al. may leave an impression that both NADPH/H_2O_2 are required for the direct conversion of coniferyl alcohol (**14**) into (−)-secoisolariciresinol (**30b**), even though there is no evidence for this. In this regard, the work should have been extended to the study of dirigent protein mediated coupling, as well as that of the enantiospecificity of the PLR in *F. koreana*, and thus of the protein/enzyme mediated steps involved. Nevertheless, these data, although lacking definitive conclusions, are generally consistent with our earlier findings using crude cell-free extracts.

This limitation in defining the actual proteins and enzymes involved has also been the case for the study of cell-free extracts of *Daphne genkwa* (Thymelaeaceae) and *Anthriscus sylvestris* (Apiaceae), which when incubated with (±)-pinoresinols (**35a/b**) in presence of NADPH, gave (−)-lariciresinol (**44b**) in 23% e.e. (Okunishi et al., 2001) and (+)-lariciresinol (**44a**)/(−)-secoisolariciresinol (**30b**) (Susuki et al., 2002a), respectively. These data would be of greater utility if the proteins/enzymes involved in these species were isolated and characterized, in order to determine the commonality to our earlier findings.

Biosynthesis of podophyllotoxin and 6-methoxypodophyllotoxin in *Linum flavum* and *Podophyllum peltatum*

Linum species

Based on the above work, it was considered that podophyllotoxin (**26**) in *Podophyllum* species (e.g., *P. peltatum*) and its 6-methoxy-derivative (**53**) in *Linum flavum* were both matairesinol (**32**) derived. [Note: previously, 6-methoxypodophyllotoxin was given the nomenclature of 5-methoxypodophyllotoxin (Dewick and Jackson, 1981; Xia et al., 2000)]. However, as regards biosynthetic pathways operative, following incubation of (±)-pinoresinols (**35a/b**) with *L. flavum* root cell-free extracts in the presence of [4*R*-^{3}H]NADPH, it was found that only (+)-pinoresinol (**35a**) was converted into (+)-[7-^{3}H]lariciresinol (**44a**) and (−)-[7,7′-^{3}H]secoisolariciresinol (**30b**), respectively (Figure 16A and 16B), as noted previously for *F. intermedia*, i.e. the corresponding enantiomer (−)-pinoresinol (**35b**) was not metabolized. Thus, no tritium was abstracted during (±)-pinoresinol (**35a/b**) reduction when the [4*S*-^{3}H] form of NADPH was employed as cofactor as above (Xia et al., 2000). Furthermore, when both (±)-[Ar-^{2}H]- and (±)-[9,9′-$^3H_2$]secoisolariciresinols (**30a/b**) were employed as substrates, the (−)-antipode (**30b**) of each was converted into (−)-[Ar-^{2}H]- and (−)-[9-^{3}H]matairesinol (**32b**), respectively. This established the existence of an intact pathway to (−)-matairesinol (**32b**) in *L. flavum* roots as for *F. intermedia* (Xia et al., 2000).

Metabolism of matairesinol (**32**) was also investigated using *L. flavum* root tissue. Following uptake and metabolism over a 6-h period, a MeOH extract was obtained, which following β-glucosidase treatment, contained a new metabolite. The latter was ultimately demonstrated to be 7′-hydroxymatairesinol (**54**) by comparison with an authentic synthetic standard (Xia et al., 2000). Figure 17 shows the mass spectral fragmentation patterns of both authentic synthetic **54** (Figure 17A) and that of the isolated 7′-hydroxymatairesinol (**54**) (Figure 17B, molecular ion at m/z 374). [7′-^{3}H]-7′-hydroxymatairesinol (**54**) was then next synthesized and administered to *L. flavum* root tissue over a 6-h period. Following metabolism as above, treatment of the resulting MeOH extract as before with β-glucosidase gave radiolabeled 6-methoxypodophyllotoxin (**53**), indicating that [7′-^{3}H]-7′-hydroxymatairesinol (**54**) was a pathway intermediate to **53**. Note, however, that beyond 7′-

hydroxymatairesinol (**54**), the stepwise conversions, including aryltetrahydronaphthalene ring formation, as well as the various hydroxylations, *O*-methylation and methylenedioxy bridge forming steps, that are required for 6-methoxypodophyllotoxin (**53**) biosynthesis are largely unknown, except for a reported *O*-methylation of β-peltatin (**55**) to give β-peltatin-A methylether (**56**) (Kranz and Petersen, 2003). Additionally, β-peltatin 6-*O*-methyltransferase was characterized in cell suspension cultures of *Linum nodiflorum*, and provisional kinetic analyses carried out on proteins recovered after $(NH_4)_2SO_4$ precipitation gave apparent K_m's of 15 and 40 μM for *S*-adenosylmethionine and β-peltatin (**55**), respectively. Other lignans, such as podophyllotoxin (**26**), matairesinol (**32**) and pinoresinol (**35**), as well as caffeic acid (**1**) were not substrates (Kranz and Petersen, 2003).

Kranz and Petersen (2003) have suggested that 6-methoxypodophyllotoxin (**53**) is not formed as described above, i.e. from 7′-hydroxymatairesinol (**54**), with these researchers suggesting that deoxypodophyllotoxin (**57**) was the common precursor of both podophyllotoxin (**26**) and 6-methoxypodophyllotoxin (**53**). In this regard, crude microsomal preparations from *L. flavum* cell suspension cultures, described as a deoxypodophyllotoxin 6-hydroxylase, introduced an hydroxyl group at the 6-position of deoxypodophyllotoxin (**57**) to form β-peltatin (**55**) (Molog et al., 2001). This preparation contained a cytochrome P-450 dependent monooxygenase, with pH and temperature optima of 7.6 and 26 °C, respectively, and apparent K_m's of 20 and 36 μM for deoxypodophyllotoxin (**57**) and NADPH, respectively. On the other hand, hydroxylation of deoxypodophyllotoxin (**57**) at the 7-position by this microsomal preparation to give podophyllotoxin (**26**) was not observed; nor was the latter hydroxylated at the 6-position to give **58** (Molog et al., 2001). These researchers also indicated that "4′-demethydeoxypodophyllotoxin (**59**) was most probably hydroxylated to α-peltatin (**60**)" while suggesting that another enzyme in the crude microsomal preparation might also be involved (Molog et al., 2001). Overall, to resolve potential ambiguities, the various proteins/enzymes truly operative in the pathway will need to be identified, with the additional caveat that if some of these enzymes display broad substrate versatility then the results obtained may not be as definitive as being proposed.

It has also been suggested, using ^{13}C-labeled precursors and *L. album* cell suspension cultures, that the initial coupling products into the lignan pathway are either two precursors with a 4-hydroxy-3-methoxy substitution pattern or alternatively only one such precursor with the other having a 3,4-methylenedioxy substitution pattern (Seidel et al., 2002). However, the data are too preliminary at this time to warrant further consideration: no chiral analysis has been carried out on coupling products and/or downstream metabolites; nor have any of the genes/enzymes involved in this putative alternate pathway been characterized and/or described. Nor has any coupling process ever been demonstrated *in vivo/in vitro* with a 3,4-methylenedioxy substitution pattern.

Podophyllum peltatum

In *Podophyllum peltatum* which forms podophyllotoxin (**26**), genes putatively encoding both the (+)-pinoresinol forming dirigent protein and SDH were obtained (Xia et al., 2000, 2001). The *P. peltatum* SDH was expressed in *E. coli* in fully functional recombinant form, and purified to apparent homogeneity. Detailed kinetic analyses, using (−)-lactol (**52b**) as substrate (Figure 14), gave K_m values ~160.2 ± 0.8 μM with an apparent maximum velocity V_{max} of ~7.1 ± 0.02 mmol/min/mg protein for (−)-matairesinol (**32b**) formation (Xia et al., 2001). The SDH was again enantiospecific, using only the (−)-antipode of secoisolariciresinol (**30b**), and not the corresponding (+)-antipode (**30a**). These data thus also confirmed the overall pathway to matairesinol (**32**) in *P. peltatum*, with the latter being considered an intermediate *en route* to podophyllotoxin (**26**). Work is now underway to determine the X-ray crystal structure of *P. peltatum* SDH, and hence to define its precise mechanistic mode of biochemical conversion.

As an additional means of investigating further the nature of transformations beyond matairesinol (**32**), [2,5,6,2′,5′,6′-$^2H_6$]matairesinol (**32**), [7′α-^{2}H]yatein (**61**) and [7′-^{2}H]podorhizol (**62**) were synthesized earlier (Neidigh et al., 1994); these, together with other potential substrates, are now being evaluated to examine which of these are involved in the remaining biochemical steps to podophyllotoxin (**26**), even though our current working hypothesis would exclude **61** and **62** unless some sort of metabolic grid was in effect. However, this will need to be fully established at the enzymatic level.

Lastly, with all genes, proteins and enzymes in hand for coniferyl alcohol (**14**) conversion to matairesinol (**32**), it is now possible to engineer levels of these lignans in various plant systems, including

Arabidopsis (model system) (Mitski et al., 2001) as well as cereal grains, such as rice (Costa et al., 1999).

Arctigenin and arctiin biosynthesis in *Forsythia intermedia*

F. intermedia accumulates the (−)-matairesinol (**32b**) derived lignans, (−)-arctigenin (**33b**) and (−)-arctiin (**34b**), which differ only in terms of either methylation of the 4′-hydroxyl group or by glycosylation at the C-4 hydroxyl group, respectively. It was of interest, therefore, to begin to establish if the *O*-methylation reactions (using crude cell-free extracts of *F. intermedia*) were capable of catalyzing either enantiospecific or regiospecific transformations (Ozawa et al., 1993). In this regard, using (±)-matairesinols (**32a/b**) as substrates, it was found that the crude OMT preparations from *F. intermedia* were neither regio- nor enantioselective, i.e. affording both (+)- and (−)-arctigenins (**33a** and **33b**) and (+)- and (−)-isoarctigenins (**63a** and **63b**) [isolated as their acetate derivatives **64a/64b** and **65a/65b**), see Scheme 5]. In both cases, however, the (−)-enantiomers were slightly preferred (*circa* 2:1) for *O*-methylation over the (+)-antipodes; no dimethylmatairesinol (**66**; Scheme 5) was obtained, indicative of discrimination occurring to prevent over (dual) methylation.

Since there are no known derivatives derived from isoarctigenin (**63**) in *F. intermedia*, our current hypothesis is that glycosylation of (−)-matairesinol (**32b**) may first occur to generate (−)-matairesinoside (**67**), with the latter then being *O*-methylated to afford (−)-arctiin (**34b**) and deglycosylated to give (−)-arctigenin (**33b**). It will be instructive in the future, however, to purify the *O*-methyltransferases in the cell-free extracts and to establish if this non-regio-/non-enantiospecific preference is truly a function of substrate versatility of the lignan forming OMT, or whether non-specific OMTs were also involved in the observed transformations.

8–8′ Allylphenol coupling and downstream metabolism in *Larrea tridentata*

Various angiosperm plant species biosynthesize allylphenol moieties (Clifford, 2000; Fisher, 1992; Gottlieb, 1972; Kollmannsberger et al., 2000), examples of which are the 8–8′ linked antiviral/anticancer lignans, nordihydroguaiaretic acid (NDGA, **68**,

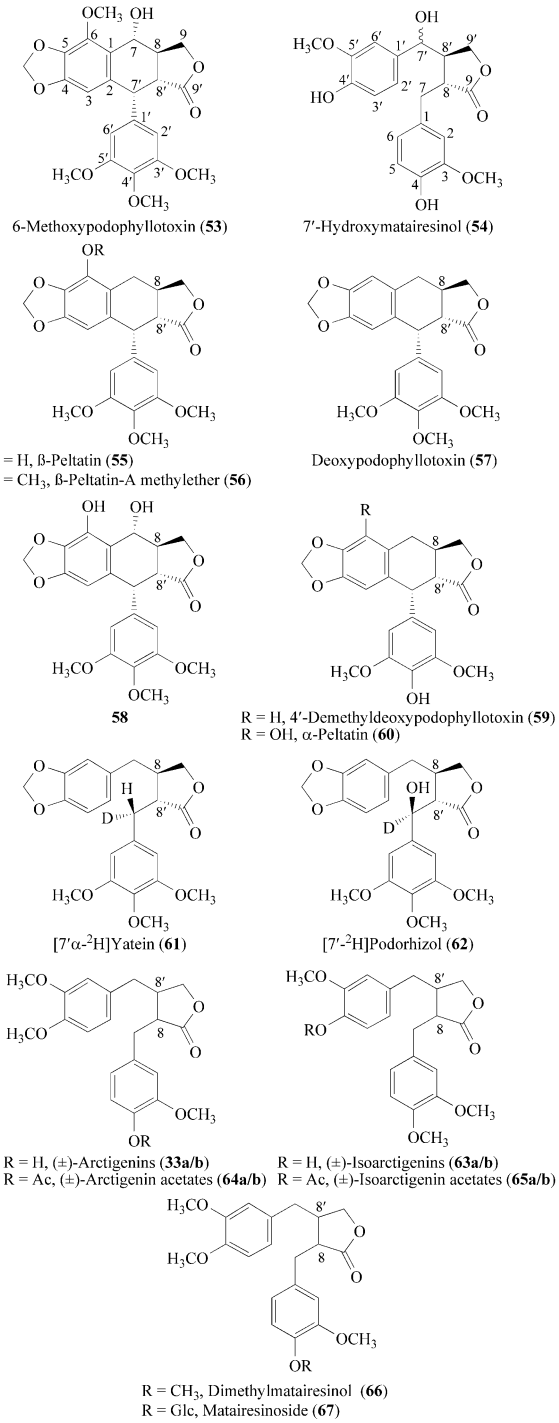

Scheme 5. Various aryltetrahydronaphthalene and dibenzylbutyrolactone lignans potentially involved in biosynthesis of podophyllotoxin (**26**) and its derivatives, and dibenzylbutyrolactone derivatives of matairesinol (**32**).

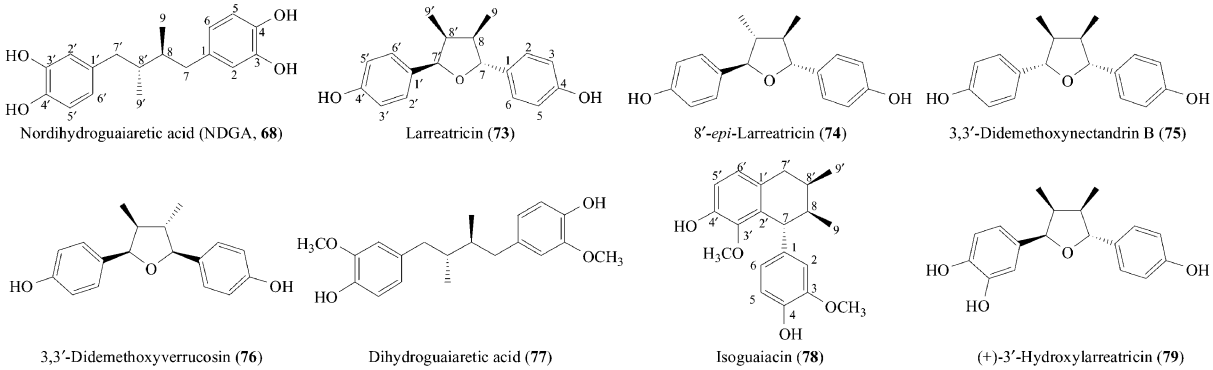

Scheme 6. Selected *Larrea tridentata* lignans.

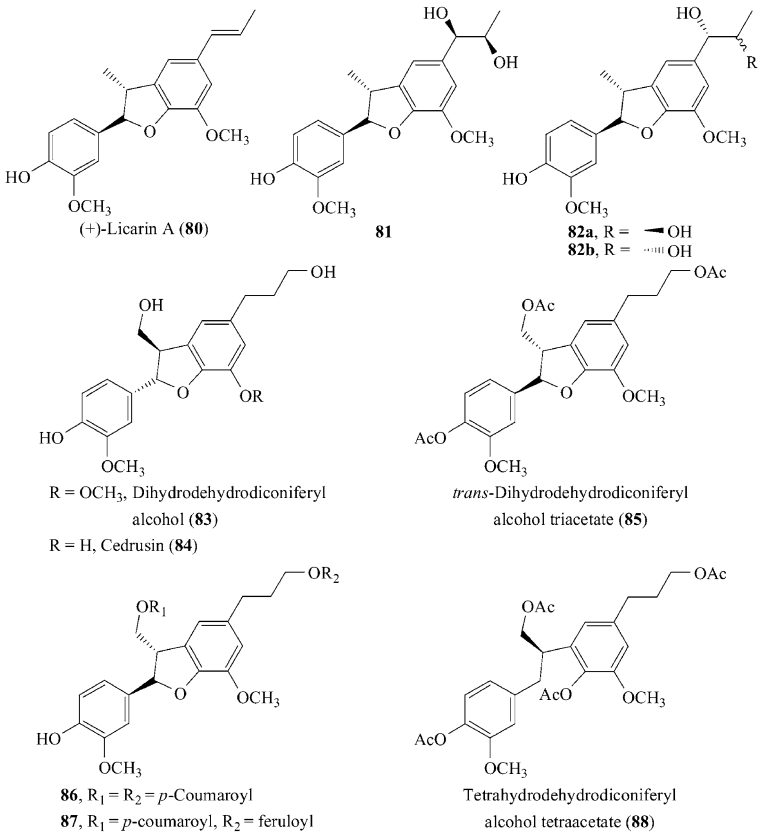

Scheme 7. Structures of various lignans.

Scheme 6) and its derivatives, from the creosote bush (*Larrea tridentata*) (Belmares et al., 1979; Craigo et al., 2000; Gnabre et al., 1995, 1996). Little is still known about how allylphenols in general are formed (other than being of phenylpropanoid origin), including the nature of the biosynthetic intermediate (or intermediates) underlying reduction (i.e., whether it is a carboxylic acid, aldehyde, alcohol or derivative thereof) as a precursor of the allylphenol group. Tracer studies using *Pimpinella anisum* cell suspension/organ cultures have been carried out to study allylphenol biosynthesis [i.e., of epoxypseudoisoeugenol-2-methylbutyrate (**69**) (Figure 18)]. A biosynthetic pathway from Phe to *p*-coumaryl alcohol (**38**), then to *p*-anol (**70**) and *E*-anethole (**71**), and finally to **69** via pseudoisoeugenol

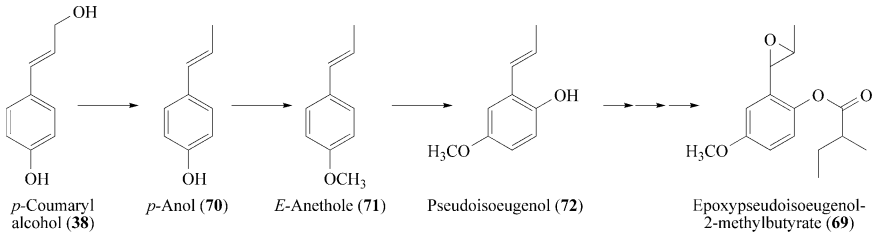

Figure 18. Proposed biosynthetic pathway to epoxypseudoisoeugenol-2-methylbutyrate (**69**) from *p*-coumaryl alcohol (**38**). Redrawn from Reichling et al. (1995b).

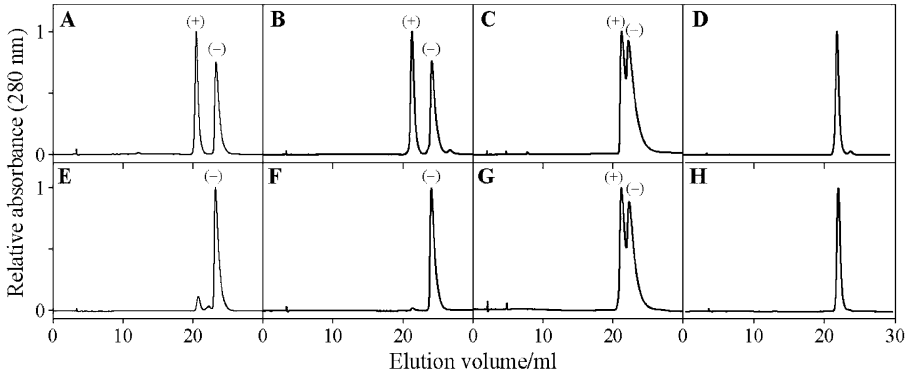

Figure 19. Chiral HPLC analysis of larreatricin (**73**), 8′-*epi*-larreatricin (**74**) and 3,3′-didemethoxyverrucosin (**76**), as well as 3,3′-didemethoxynectandrin B (**75**). Upper panel: chiral HPLC separation of synthetic (±) stereoisomers **73**, **74** and **76** (upper panels A, B and C). Panel D shows elution profile of *meso*-didemethoxynectandrin B (**75**). Lower panel: chiral HPLC analysis of naturally occurring *L. tridentata* lignans **73**–**76** (lower panels). Redrawn from Moinuddin et al. (2003). See Scheme 6 for structures.

(**72**) (see Figure 18) was proposed, but without unambiguously identifying the enzymes/proteins involved (Kemmerer and Reichling, 1996; Reichling et al., 1995a,b)

In *L. tridentata*, the simplest lignans (structurally), and presumed to represent the initial coupling products, are those apparently derived from *p*-anol (**70**) radical-radical coupling, i.e., the dibenzyltetrahydrofuran 8–8′ linked larreatricin (**73**), 8′-*epi*-larreatricin (**74**), 3,3′-didemethoxynectandrin B (**75**) and 3,3′-didemethoxyverrucosin (**76**) (Scheme 6). This plant species, however, also biosynthesizes a plethora of other lignans, all 8–8′ linked, including dibenzylbutanes [e.g., NDGA (**68**) and dihydroguaiaretic acid (**77**)] and aryltetrahydronaphthalenes [e.g., isoguaiacin (**78**)]. All of these other natural products can also be considered to result from *p*-anol (**70**) coupling products, following various oxidative and/or reductive transformations. [Of these 8–8′ lignans, however, the most abundant is NDGA (**68**).]

The isolation of the presumed initial *p*-anol (**70**) coupling products, **73**–**76**, gave some interesting findings when subjected to chiral HPLC analysis; it was found that both larreatricin (**73**) and 8′-*epi*-larreatricin (**74**) existed essentially in pure enantiomeric form, whereas 3,3′-didemethoxynectandrin B (**75**) and (±)-3,3′-didemethoxyverrucosins (**76**) were in their *meso* and racemic forms, respectively. This was unambiguously demonstrated by first synthesizing **73**–**76** in racemic and *meso* forms and subjecting **73**, **74** and **76** to chiral HPLC enantiomeric resolution, with these being compared to the chiral HPLC-traces of the isolated lignans (Figure 19) (Moinuddin et al., 2003). The presence of **73**–**76** thus suggested that either regiospecific coupling was occurring to (i) generate racemic (±)-8–8′ linked **73**, **74** and **76** and the *meso* compound **75**, with the (+)-enantiomers of **73** and **74** enantiospecifically undergoing further metabolism, or that (ii) (−) **73** and (−) **74** were being formed via stereoselective coupling. However, a subsequent study of the biosynthetic pathway to NDGA (**68**) resolved this question, in which a polyphenol oxidase (MW ∼ 33 kDa) was isolated capable of enantiospecifically hydroxylating (+)-larreatricin (**73**) primarily at the 3′-position to generate (+)-3′-hydroxylarreatricin (**79**); by contrast the (−)-antipode was not hydroxylated (Figure 20) (Cho et al., 2003). The gene encoding the corresponding protein, (upon the latter's purifica-

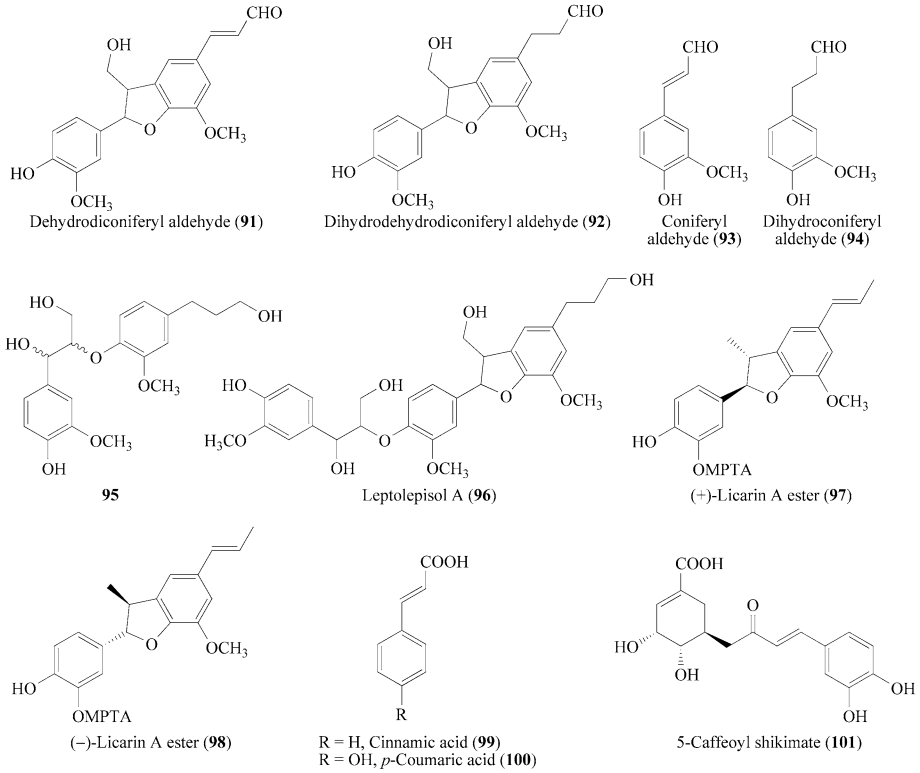

Scheme 8. Structures of various lignans, hydroxycinnamyl aldehydes/acids and derivatives thereof.

tion to apparent homogeneity) was then cloned, and was found to encode a polyphenol oxidase (PPO), of ∼61 kDa rather than the ∼43 kDa protein isolated. However, the smaller size of the latter is due to post-translation processing, a well-known phenomena with PPOs (Cho et al., 2003). Interestingly, the (+)-larreatricin hydroxylase contains two highly conserved PPO copper binding domains A and B. Studies are currently underway to establish the biochemical mechanisms associated with this first example of PPO enantiospecificity, e.g. through X-ray crystallization of the post-translationally processed PPO containing the bound substrate(s). Additional work is also being directed as to how 8–8′ regiospecific coupling is occurring at the biochemical level, given that only 8–8′-linked lignans have been isolated from this species and that other bonding types (e.g. 8–5′, 8–*O*–4′) have not been detected in either metabolism or isolation studies.

8–5′, 8–*O*–4′ and 8–2′ linked lignans

Many of the lignans present in vascular plants have linkages other than 8–8′ and, of these, the bulk of the biochemical work has thus far been directed towards elucidating mechanisms of 8–5′, 8–*O*–4′ and 8–2′ linked lignan formation.

8–5′ and 8–O–4′ linked lignans

Most 8–5′ linked lignans are apparently dehydrodiconiferyl alcohol (**21**) derived (Lewis and Davin, 1999), and can exist in a wide variety of structural forms. Other analogues, such as (+)-licarin A (**80**) and the two related diols **81** and **82a/b**, are apparently allylphenol-derived (Nascimento and Lopes, 1999; Nascimento et al., 2000). Of the dehydrodiconiferyl alcohol (**21**) derived lignans, these include allylic double bond reduced derivatives at positions 7′,8′ [e.g., dihydrodehydrodiconiferyl alcohol (**83**) and its demethyl analogues, such as cedrusin (**84**) from *Pinus taeda* (Gang et al., 1999b; Nose et al., 1995), the corresponding triacetate (**85**) from *Cryptomeria japonica* (Su et al., 1995) as well as various *p*-coumaroyl and

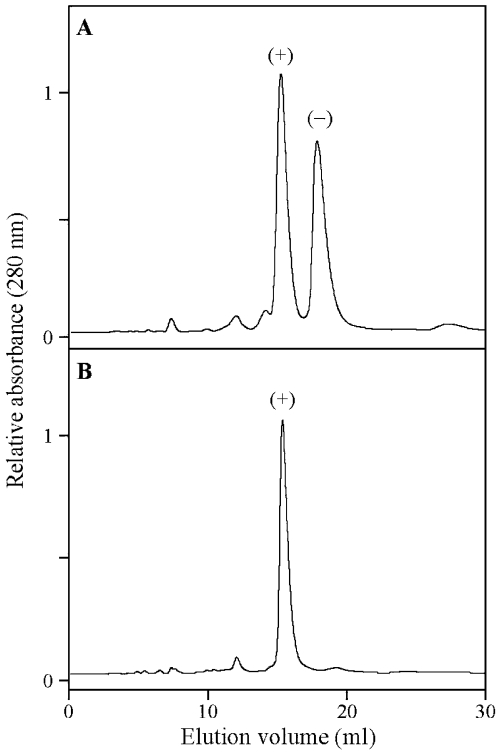

Figure 20. Enantiospecificity of (+)-larreatricin 3′-hydroxylase. (**A**) Chiral separation of synthetic (+)- and (−)-3′-hydroxylarreatricins (**79**) and (**B**) enantiomeric composition of enzymatically formed 3′-hydroxylarreatricin (**79**). Redrawn from Cho et al. (2003).

feruloyl derivatives, e.g. **86** and **87** from *Corylus sieboldiana* (Watanabe et al., 1992)]. In addition, there are a number of other lignan derivatives which have apparently resulted from 7–*O*–4′ bond cleavage, e.g., to afford 8–5′ linked diaryl derivatives such as compound **88** from *C. japonica* (Su et al., 1995); all of these lignan skeleta are apparently coniferyl alcohol (**14**) derived (Lewis and Davin, 1999).

We have placed considerable emphasis upon defining the processes involved in both 7–*O*–4′ bond cleavage and 7′,8′-allylic double bond reductions, much of which is now understood at the gene and enzyme levels (Gang et al., 1999b; Kasahara et al., 2003, 2004; Min et al., 2003).

Phenylcoumaran benzylic ether reductase (PCBER)

The 7–*O*–4′ bond reduction occurs via involvement of a phenylcoumaran benzylic ether reductase (PCBER), with the corresponding recombinant 33.6 kDa protein first obtained following cloning of the encoding gene from *P. taeda* (Gang et al., 1999b). This recombinant enzyme, as well as a *Populus trichocarpa* analogue, were able to relatively slowly catalyze 7–*O*–4′ reductions of both (±)-dehydrodiconiferyl (**21**) and (±)-dihydrodehydrodiconiferyl (**83**) alcohols in a regiospecific, but not enantiospecific, manner to afford (±)-isodihydrodehydrodiconiferyl alcohols (**89**) and (±)-tetrahydrodehydrodiconiferyl alcohols (**90**), respectively (Figure 21). As for the PLRs previously described, the PCBER also abstracts the 4*R*-hydride from NADPH during catalysis (Gang et al., 1999b). Interestingly, PCBERs, PLRs and isoflavone reductase(s) (IFRs) are quite closely related from a sequence homology perspective, i.e. PCBER is ∼66% similar/∼45% identical to PLRs and ∼65% similar/∼50% identical to IFRs. In this regard, this level of homology has led to the suggestion that PCBER (being regiospecific) is the evolutionary forerunner of the enantiospecific PLRs and IFRs (Gang et al., 1999b).

The X-ray structures of PLR and PCBER have recently been reported and that of IFR modeled (Min et al., 2003), with the three-dimensional X-ray crystal structure of PCBER_Pt1 solved and refined to 2.2 Å resolution. Its overall gross structure is composed of two domains (N-terminal and C-terminal) connected by five separate peptide segments, with the two domains forming a cleft between them as for PLR_Tp1. The putative cofactor-binding site in PCBER_Pt1 (as for PLR_Tp1 and modeled IFR) was identified so that the nicotinamide ring is orientated towards the cleft between the two domains. Since PCBER only abstracts the 4-*pro*-*R*-hydride from the *re*-side of the dihydronicotinamide ring of NADPH, the mechanism for NADPH binding is best satisfied whereby the nicotinamide ring fits into an *anti*-conformation (Figure 15D). As for PLR_Tp1, the dehydrodiconiferyl alcohol (**21**) binding pocket is made up of two β-strands and two α-helical segments (Figure 15C) including the conserved lysine residue (Lys^{134}) involved in general base catalysis, and is adjacent to the cofactor. PCBER regiospecificity is best explained by a larger space (when compared to that in PLR_Tp1) in the substrate binding pocket where both (+)- and (−)-dehydrodiconiferyl alcohols (**21a/b**) can fit among the hydrophobic side chains of Phe^{160}, Ser^{263} and Ser^{267} (Figure 15C) (Min et al., 2003).

Polyclonal antibodies specific to PCBER were also prepared and used to define the cellular and tissue specificities of PCBER in *P. taeda* newly growing shoots and woody stem tissues, respectively (Kwon et al., 2001). At the new shoot developmental stage,

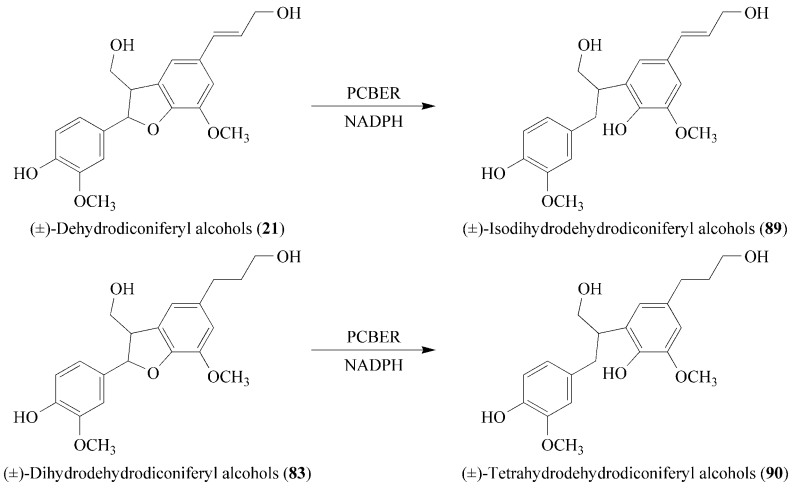

Figure 21. Reactions catalyzed by PCBER.

PCBER was localized in the differentiating secondary xylem regions (i.e. in areas containing undifferentiated tracheids and fibers, as well as initials of both axial and radial parenchyma cells). In the mature woody stem tissue, PCBER was localized in fully differentiated axial and radial parenchyma cells, and to a much lesser extent in the vascular cambium (i.e., axial and/or radial parenchyma cell initials). In summary, PCBER was mainly localized in the radial and axial parenchyma cells of *P. taeda*; somewhat analogous findings for PCBER have been reported for poplar (Vander Mijnsbrugge et al., 2000). These data, in turn, are in accordance with the role of these metabolites in both defense and in heartwood and/or sapwood forming processes. Furthermore, PCBER displays minor allergenic properties (e.g. in birch pollen, as well as in various fruits and vegetables), suggesting yet another role in plant defense (Karamloo et al., 2001).

Aryl propenal double bond reductases

A regiospecific aryl propenal double bond reductase (APDBR) capable of converting both (+)- and (−)-enantiomers of dehydrodiconiferyl aldehyde (**91**) into (+)- and (−)-dihydrodehydrodiconiferyl aldehydes (**92**), as well as coniferyl aldehyde (**93**) into dihydroconiferyl aldehyde (**94**)(Figure 22), was isolated from *Pinus taeda*, and purified to apparent homogeneity; its encoding gene was cloned, and the fully functional recombinant APBDR obtained (Kasahara et al., 2003, 2004). The ∼39 kDa enzyme abstracts the 4*R*-hydride from NADPH (Kasahara et al., 2003, 2004), and the pathway, using dehydrodiconiferyl alcohol (**21**) as an example, first involves initial oxidation

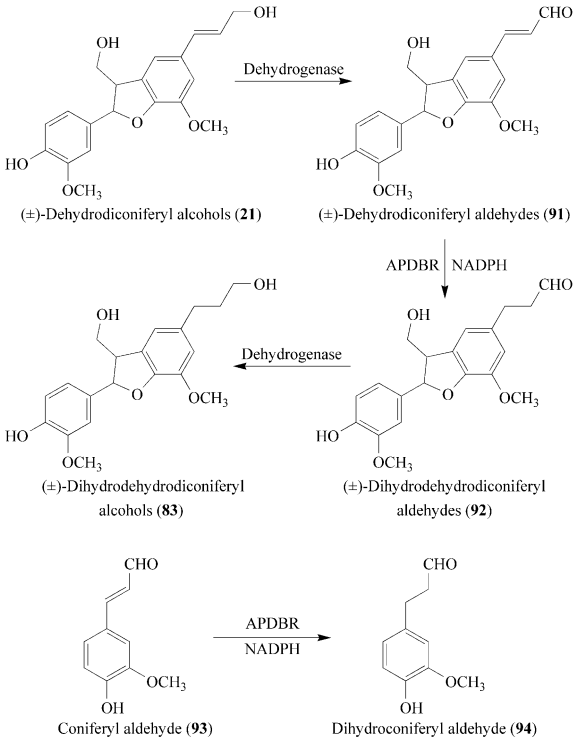

Figure 22. Catalytic action of *P. taeda* arylpropenal double bond reductase (APDBR).

of the terminal allylic hydroxyl group by a dehydrogenase to give **91**, with regiospecific reduction of the side-chain to generate the corresponding dihydro analogue **92** which is then reduced back to afford lignan **83** (Figure 22). The same enzyme is also presumed to be involved in converting the 8–*O*–4′

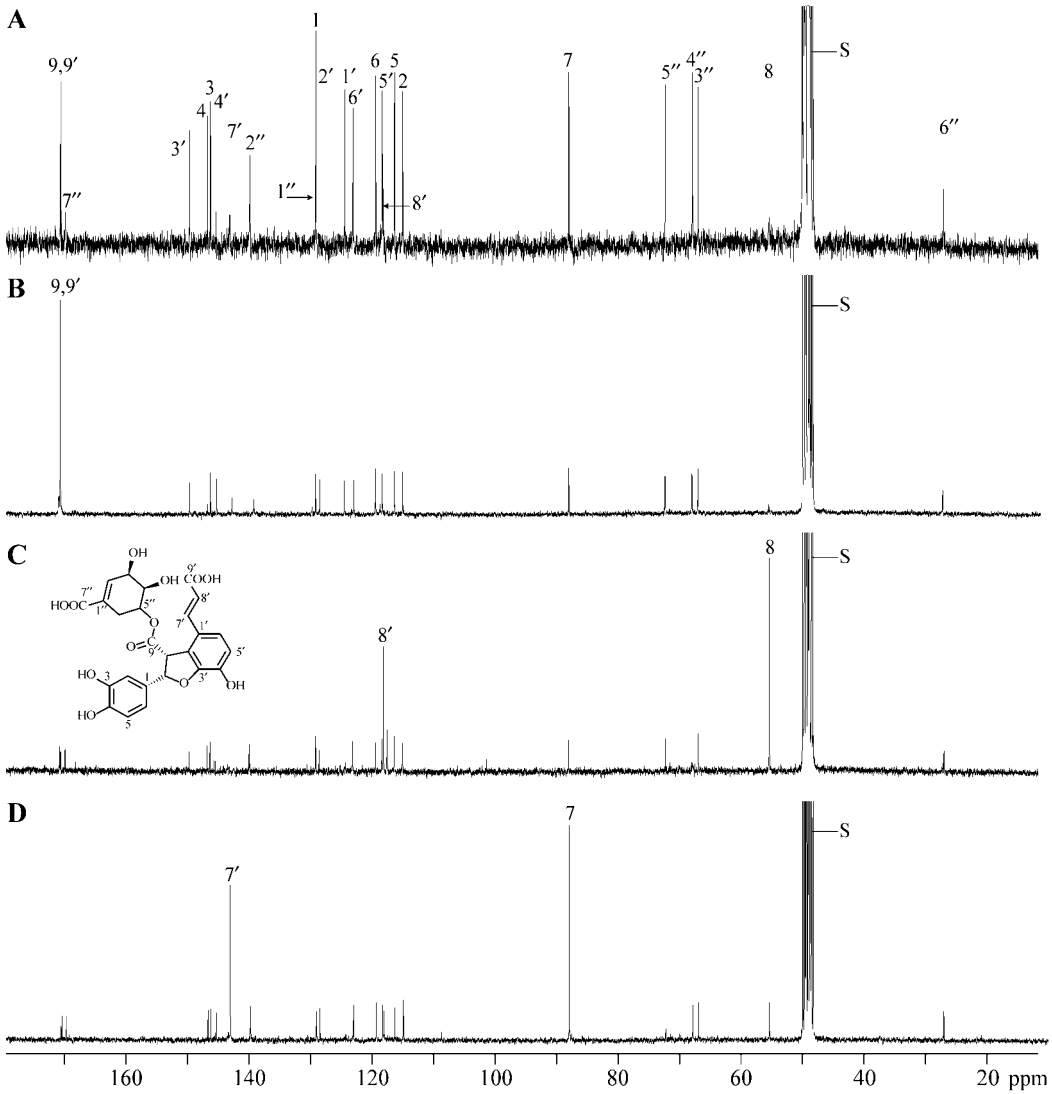

Figure 23. ^{13}C-NMR spectra of (**A**) natural abundance (−)-brainic acid (**17**), as well as (−)-brainic acids (**17**) obtained following administration of (**B**) [1-^{13}C], (**C**) [2-^{13}C] and (**D**) [3-^{13}C]-phenylalanine (1 mM) to *B. spicant* fronds for 5 days; all spectra were recorded under identical conditions (Davin et al., 2003). [*S* =Solvent]

analogs in *Pinus* species into the corresponding dihydro species, e.g., **95** from *Pinus massoniana* (Lundgren et al., 1985). The enzymology associated with 8–*O*–4′ linkage formation is also currently under investigation, as are the dehydrogenases involved in the oxidative/reductive steps of the allylic/propanyl alcohol functionalities (see Figure 22).

Interestingly, three proteins having phenylpropanoid aryl propenal double bond reductase properties have also been obtained from *Arabidopsis thaliana* (Kim et al., manuscript in preparation) with members capable of reducing both phenylpropanoid monomers (hydroxycinnamic acids, hydroxycinnamyl aldehydes and hydroxycinnamyl alcohols) to afford the corresponding 7,8 double bond reduced substances, as well as also acting on 8–5′ lignans, such as dehydrodiconiferyl aldehyde (**91**).

In situ hybridization of APDBR has been conducted in young *P. taeda* stem tissues at two development stages, i.e. in the meristematic region and the woody tissue of a 1 year-old stem, with digoxigenin-labeled antisense and sense (control) RNA probes being synthesized. It was thus found that APDBR was primarily localized in both the axial and ray parenchyma cells,

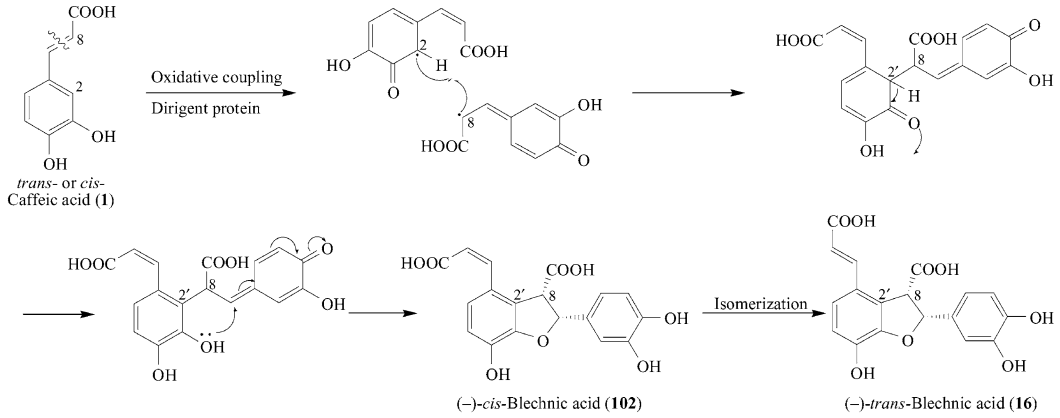

Figure 24. Proposed stereoselective coupling of caffeic acid (**1**) leading to (−)-*trans*-blechnic (**16**).

and to a lesser extent in the cambial regions (Kasahara et al., 2004).

From a physiological perspective, various dihydrophenylpropanoid monomeric and dimeric compounds have been shown to be present in the Pinaceae, e.g. *Picea glauca*, as part of defense response (Kraus and Spiteller, 1997). They are also converted into various oligomeric forms, such as leptolepisol A (**96**) in *Larix leptolepis* (Sakakibara et al., 1987). Thus, their generation is not part of lignin assembly (used for sapwood formation) but instead they are part of the heartwood defense chemical armoury (Sakakibara et al., 1987); additionally, in *P. glauca* their formation is inducible, e.g. by the gall aphid *Adelges abietis* (Kraus and Spiteller, 1997).

8–5′ linked allylphenol lignans

As indicated earlier, *Aristolochia pubescens* accumulates the lignans (+)-licarin A (**80**) and the two diols **81** and **82a/b** (Nascimento and Lopes, 1999), and synthetic processes have been developed to obtain (+)- and (−)-licarin A ester derivatives **97/98** in enantiomerically pure form (Nascimento et al., 2000). Work is currently underway to define the enzymology/protein chemistry involved in both their coupling reactions and in their downstream metabolic conversions.

8–2′ linked lignans

The lignans *trans*-blechnic acid (**16**) and *trans*-brainic (**17**) acids are two 8–2′ linked metabolites found in the Pteridophytes, specifically *Blechnum orientale* (Wada et al., 1992) and *Blechnum spicant* (Davin et al., 2003; Wang et al., 2001). Radiolabeling administration experiments using *B. spicant* fronds, with potential precursors, L-[U-^{14}C]Phe, L-[U-^{14}C]Tyr, [2-^{14}C]acetate, [9-^{14}C] cinnamate (**99**) and [8-^{14}C]-*p*-coumarate (**100**), revealed that all (except for [U-^{14}C]-Tyr and [2-^{14}C]-acetate) were individually incorporated into caffeic acid (**1**), 5–*O*–caffeoyl shikimate (**101**), (−)-*trans*-blechnic acid (**16**) and (−)-*trans*-brainic acid (**17**), respectively (Davin et al., 2003; Wang et al., 2001). These initial studies were both confirmed and extended following the individual uptake and metabolism of [1-^{13}C], [2-^{13}C] and [3-^{13}C]Phe to *B. spicant* fronds over a 5 day period, which established intact incorporation into lignans, (−)-brainic acid (**17**) (Figure 23) and (−)-blechnic acid (**16**) (data not shown). In each case, the lignan of interest was isolated and subjected to ^{13}C NMR spectroscopic analysis.

Figure 23A shows the natural abundance ^{13}C NMR spectrum of (−)-brainic acid (**17**), whereas Figure 23B-D display the spectra showing enhanced resonances at 9,9′ (Figure 23B), 8–8′ (Figure 23C) and 7,7′ (Figure 23D), thereby demonstrating intact incorporation of the various [^{13}C]labeled Phe precursors. While the corresponding gene(s), proteins/enzymes involved in (−)-blechnic (**16**)/(−)-brainic (**17**) acid formation have not yet been isolated, a mechanism involving stereoselective coupling of caffeic acid (**1**) can be provisionally proposed (Figure 24). Ongoing work is underway to delineate the precise biochemical processes operative and which control stereoselective hydroxycinnamic acid coupling.

Concluding remarks

While much is now known about lignan biosynthesis (particularly of the 8–8′ and 8–5′ linked compounds),

much remains to be determined. This includes defining mechanistic questions regarding the action of dirigent proteins (i.e. in terms of binding, orientation and coupling), as well as in establishing further the molecular basis of enantioselectivity of downstream enzymatic steps in lignin metabolism. Much also remains to be done in clarifying the nature of additional biochemical transformations to complex lignan molecules, such as podophyllotoxin (**26**), leptolepisol A (**96**), plicatic acid (**20**) and so forth; these will be the subject of future work, as will defining further the mechanisms of macromolecular assembly of lignin and suberin biopolymers.

Acknowledgements

This work was supported by the National Science Foundation (MCB9976684), the National Aeronautics and Space Administration (NAG 2-1513), the National Institute of General Medical Sciences (5 R01 GM066173-02), the United States Department of Energy (DE FG03-97ER20259), McIntire Stennis, and the G. Thomas and Anita Hargrove Center for Plant Genomic Research.

References

Belmares H, Barrera A, Castillo E, Ramos LF, Hernandez F & Hernandez V (1979) New rubber antioxidants and fungicides derived from *Larrea tridentata* (creosote bush). Ind. Eng. Chem. Prod. Res. Dev. 18: 220–226.

Bakke JE & Klosterman HS (1956) A new diglucoside from flaxseed. Proc. No. Dakota Acad. Sci. 10: 18–22.

Borriello SP, Setchell KDR, Axelson M & Lawson AM (1985) Production and metabolism of lignans by the human fecal flora. J. Appl. Bacteriol. 58: 37–43.

Burlat V, Kwon M, Davin LB & Lewis NG (2001) Dirigent proteins and dirigent sites in lignifying tissues. Phytochemistry 57: 883–897.

Cho M-H, Moinuddin SGA, Helms GL, Hishiyama S, Eichinger D, Davin LB & Lewis NG (2003) (+)-Larreatricin hydroxylase, an enantio-specific polyphenol oxidase from the creosote bush (*Larrea tridentata*). Proc. Natl. Acad. Sci., USA 100: 10641–10646.

Chu A, Dinkova A, Davin LB, Bedgar DL & Lewis NG (1993) Stereospecificity of (+)-pinoresinol and (+)-lariciresinol reductases from *Forsythia intermedia.* J. Biol. Chem. 268: 27026–27033.

Clark AM, El-Feraly FS & Li W-S (1981) Antimicrobial activity of phenolic constituents of *Magnolia grandiflora* L. J. Pharm. Sci. 70: 951–952.

Clifford MN (2000) Miscellaneous phenols in foods and beverages – nature, occurrence and dietary burden. J. Sci. Food Agr. 80: 1126–1137.

Costa MA, Xia Z-Q, Davin LB & Lewis NG (1999) Toward engineering the metabolic pathways of cancer-preventing lignans in cereal grains and other crops. In: Romeo JT (ed) Recent Advances in Phytochemistry, Vol 33 (pp. 67–87). Kluwer Academic/Plenum Publishers, New York.

Craigo J, Callahan M, Huang RCC & DeLucia AL (2000) Inhibition of human papillomavirus type 16 gene expression by nordihydroguaiaretic acid plant lignan derivatives. Antiv. Res. 47: 19–28.

Croteau R, Kutchan TM & Lewis NG (2000) Natural products (secondary metabolites). In: Buchanan BB, Gruissem W & Jones RL (eds), Biochemistry and Molecular Biology of Plants (pp. 1250–1318). American Society of Plant Physiologists, Rockville, MD.

Cullmann F, Adam K-P & Becker H (1993) Bisbibenzyls and lignans from *Pellia epiphylla.* Phytochemistry 34: 831–834.

Cullmann F, Adam K-P, Zapp J & Becker H (1996) Pelliatin, a macrocyclic lignan derivative from *Pellia epiphylla.* Phytochemistry 41: 611–615.

Davin L, Umezawa T & Lewis NG (1990) Biosynthesis of *Forsythia* lignans. Bull. Liaisons Groupe Polyphénols 15: 96–99.

Davin LB, Bedgar DL, Katayama T & Lewis NG (1992) On the stereoselective synthesis of (+)-pinoresinol in *Forsythia suspensa* from its achiral precursor, coniferyl alcohol. Phytochemistry 31: 3869–3874.

Davin LB & Lewis NG (1992) Phenylpropanoid metabolism: biosynthesis of monolignols, lignans and neolignans, lignins and suberins. In: Stafford HA & Ibrahim RK (eds), Recent Advances in Phytochemistry, Vol 26 (pp. 325–375). Plenum Press, New York.

Davin LB, Wang H-B, Crowell AL, Bedgar DL, Martin DM, Sarkanen S & Lewis NG (1997) Stereoselective bimolecular phenoxy radical coupling by an auxiliary (dirigent) protein without an active center. Science 275: 362–366.

Davin LB & Lewis NG (2000) Dirigent proteins and dirigent sites explain the mystery of specificity of radical precursor coupling in lignan and lignin biosynthesis. Plant Physiol. 123: 453–461.

Davin LB, Wang C-Z, Helms GL & Lewis NG (2003) [^{13}C]-Specific labeling of 8–2′ linked (−)-*cis*-blechnic, (−)-*trans*-blechnic and (−)-brainic acids in the fern *Blechnum spicant.* Phytochemistry 62: 501–511.

Dewick PM & Jackson DE (1981) Cytotoxic lignans from *Podophyllum*, and the nomenclature of aryltetralin lignans. Phytochemistry 20: 2277–2280.

Dewick PM (1990) Biosynthesis of lignans. In: Atta-ur-Rahman (ed) Studies in Natural Product Chemistry, Vol 5 (pp. 459–503). University of Karachi, Karachi, Pakistan.

Dinkova-Kostova AT, Gang DR, Davin LB, Bedgar DL, Chu A & Lewis NG (1996) (+)-Pinoresinol/(+)-lariciresinol reductase from *Forsythia intermedia*: protein purification, cDNA cloning, heterologous expression and comparison to isoflavone reductase. J. Biol. Chem. 271: 29473–29482.

Droz JP & Rivoire M (2001) Advanced testis cancer. Curr. Treat. Options Oncol. 2: 421–429.

Fisher C (1992) Phenolic compounds in spices. In: Ho C-T, Lee CY & Huang M-T (eds), Phenolic Compounds in Food and their Effects on Health, I, Analysis, Occurence and Chemistry, Vol 506 (pp. 118–129). ACS Symposium Series, Washington, DC.

Ford CW & Hartley RD (1990) Cyclodimers of *p*-coumaric and ferulic acids in the cell walls of tropical grasses. J. Sci. Food Agric. 50: 29–43.

Ford JD, Davin LB & Lewis NG (1999) Plant lignans and health: cancer chemoprevention and biotechnological opportunities. In: Gross GG, Hemingway RW & Yoshida T (eds), Plant Polyphenols 2: Chemistry, Biology, Pharmacology, Ecology (pp. 675–694). Kluwer Academic/Plenum Publishers, New York.

Ford JD, Huang K-S, Wang H-B, Davin LB & Lewis NG (2001) Biosynthetic pathway to the cancer chemopreventive secoisolari-

ciresinol diglucoside-hydroxymethyl glutaryl ester-linked lignan oligomers in flax (*Linum usitatissimum)* seed. J. Nat. Prod. 64: 1388–1397 and 65: 800.

Fujita M, Gang DR, Davin LB & Lewis NG (1999) Recombinant pinoresinol/lariciresinol reductases from western red cedar (*Thuja plicata*) catalyze opposite enantiospecific conversions. J. Biol. Chem. 274: 618–627.

Gang DR, Dinkova-Kostova AT, Davin LB & Lewis NG (1997) Phylogenetic links in plant defense systems: lignans, isoflavonoids and their reductases. In: Hedin PA, Hollingworth RM, Masler EP, Miyamoto J & Thompson DG (eds), Phytochemical Pest Control Agents, Vol 658 (pp. 58–89). ACS Symposium Series, Washington, DC.

Gang DR, Costa MA, Fujita M, Dinkova-Kostova AT, Wang H-B, Burlat V, Martin W, Sarkanen S, Davin LB & Lewis NG (1999a) Regiochemical control of monolignol radical coupling: a new paradigm for lignin and lignan biosynthesis. Chem. Biol. 6: 143–151.

Gang DR, Kasahara H, Xia Z-Q, Vander Mijnsbrugge K, Bauw G, Boerjan W, Van Montagu M, Davin LB & Lewis NG (1999b) Evolution of plant defense mechanisms: relationships of phenylcoumaran benzylic ether reductases to pinoresinol-lariciresinol and isoflavone reductases. J. Biol. Chem. 274: 7516–7527.

Gardner JAF, MacDonald BF & MacLean H (1960) The polyoxyphenols of western red cedar (*Thuja plicata* Donn). II. Degradation studies on plicatic acid, a possible lignan acid. Can. J. Chem. 38: 2387–2394.

Gardner JAF, Swan EP, Sutherland SA & MacLean H (1966) Polyoxyphenols of western red cedar (*Thuja plicata* Donn) III. Structure of plicatic acid. Can. J. Chem. 44: 52–58.

Glossmann J-P, Josting A & Diehl V (2002) New treatments for Hodgkin's disease. Curr. Treat. Options Oncol. 3: 283–290.

Gnabre JN, Brady JN, Clanton DJ, Ito Y, Dittmer J, Bates RB & Huang RCC (1995) Inhibition of human immunodeficiency virus type 1 transcription and replication by DNA sequence-selective plant lignans. Proc. Natl. Acad. Sci. USA 92: 11239–11243.

Gnabre JN, Ito Y, Ma Y & Huang RC (1996) Isolation of anti-HIV-1 lignans from *Larrea tridentata* by counter-current chromatography. J. Chromatogr., A 719: 353–364.

Gottlieb OR (1972) Chemosystematics of the Lauraceae. Phytochemistry 11: 1537–1570.

Gottlieb OR (1978) Neolignans. Progress in the Chemistry of Organic Natural Products 35: 1–72.

Gottlieb OR & Yoshida M (1989) Lignans. In: Wand J & Kirk CH (eds), Natural Products of Woody Plants – Chemical Extraneous to the Lignocellulosic Cell Wall (pp. 439–511). Springer Verlag, Berlin.

Hainsworth JD (1999) Extended-schedule oral etoposide in selected neoplasms and overview of administration and scheduling issues. Drugs 58 (Suppl. 3): 51–56.

Halls SC & Lewis NG (2002) Secondary and quaternary structures of the (+)-pinoresinol forming dirigent protein. Biochemistry 41: 9455–9461.

Halls SC & Lewis NG (2003) Reversed-phase HPLC lignan chiral analysis with laser polarimetric detection. Tetrahedron Assym. 14: 649–658.

Halls SC, Davin LB, Kramer DM & Lewis NG (2004) A kinetic study of coniferyl alcohol radical binding to the (+)-pinoresinol forming dirigent protein. Biochemistry 43: 2587–2595.

Hande KR (1998) Etoposide: four decades of development of a topoisomerase II inhibitor. Eur. J. Cancer 34: 1514–1521.

Hartley RD & Ford CW (1989) Phenolic constituents of plant cell walls and wall biodegradability. In: Lewis NG & Paice MG (eds), Plant Cell Wall Polymers. Biogenesis and Biodegradation, Vol 399 (pp. 137–145). ACS Symposium Series, Washington, DC.

Hartwell JL & Schrecker AW (1951) Components of podophyllin. V. The constitution of podophyllotoxin. J. Am. Chem. Soc. 73: 2909–2916.

Hartwell JL & Schrecker AW (1958) Chemistry of podophyllum. Fortsch. Chem. Org. Naturstoffe 15: 83–166.

Jackson DE & Dewick PM (1984) Biosynthesis of *Podophyllum* lignans. I. Cinnamic acid precursors of podophyllotoxin in *Podophyllum hexandrum.* Phytochemistry 23: 1029–1035.

Jenab M & Thompson LU (1996) The influence of flaxseed and lignans on colon carcinogenesis and β-glucuronidase activity. Carcinogenesis 17: 1343–1348.

Jiao Y, Davin LB & Lewis NG (1998) Furanofuran lignan metabolism as a function of seed maturation in *Sesamum indicum*: methylenedioxy bridge formation. Phytochemistry 49: 387–394.

Johansson CI, Saddler JN & Beatson RP (2000) Characterization of the polyphenolics related to the colour of western red cedar (*Thuja plicata* Donn) heartwood. Holzforschung 54: 246–254.

Kamal-Eldin A, Peerlkamp N, Johnsson P, Andersson R, Andersson RE, Lundgren LN & Åman P (2001) An oligomer from flaxseed composed of secoisolariciresinol diglucoside and 3-hydroxy-3-methyl glutaric acid residues. Phytochemistry 58: 587–590.

Kamil WM & Dewick PM (1986) Biosynthesis of the lignans α- and β-peltatin. Phytochemistry 25: 2089–2092.

Karamloo F, Wangorsch A, Kasahara H, Davin LB, Haustein D, Lewis NG & Vieths S (2001) Phenylcoumaran benzylic ether and isoflavonoid reductases are a new class of cross-reactive allergens in birch pollen, fruits, nuts and vegetables. Eur. J. Biochem. 268: 5310–5320.

Kasahara H, Davin LB & Lewis NG (2003) Cloning and sequence of aryl propenal double bond reductase from loblolly pine and construction of transgenic plant expressing the enzyme. U.S. Pat. Appl. Publ. (US 2003022168) Priority: US 2000-192266 20000327: 17 pp.

Kasahara H, Jiao Y, Bedgar DL, Patten AM, Xia X-Q, Davin LB & Lewis NG (2004) Relationship of a *Pinus taeda* aryl propenal double-bond reductase to lignan and lignin biosynthesis: Purification, cDNA cloning and heterologous expression in *Escherichia coli* and characterization. (Manuscript in preparation).

Katayama T, Davin LB & Lewis NG (1992) An extraordinary accumulation of (−)-pinoresinol in cell-free extracts of *Forsythia intermedia*: evidence for enantiospecific reduction of (+)-pinoresinol. Phytochemistry 31: 3875–3881.

Katayama T, Davin LB, Chu A & Lewis NG (1993) Novel benzylic ether reductions in lignan biogenesis in *Forsythia intermedia.* Phytochemistry 33: 581–591.

Kato MJ, Chu A, Davin LB & Lewis NG (1998) Biosynthesis of antioxidant lignans in *Sesamum indicum* seeds. Phytochemistry 47: 583–591.

Kelly MG & Hartwell JL (1954) The biological effects and the chemical composition of podophyllin. A review. J. Nat. Cancer Inst. 14: 967–1010.

Kemmerer B & Reichling J (1996) *S*-Adenosyl-L-methionine: anol-*O*-methyltransferase activity in organ cultures of *Pimpinella anisum.* Phytochemistry 42: 397–403.

Kim MK, Jeon J-H, Davin LB & Lewis NG (2002a) Monolignol radical-radical coupling networks in western red cedar and *Arabidopsis* and their evolutionary implications. Phytochemistry 61: 311–322.

Kim MK, Jeon J-H, Fujita M, Davin LB & Lewis NG (2002b) The western red cedar (*Thuja plicata*) 8–8′ *DIRIGENT* family displays diverse expression patterns and conserved monolignol coupling specificity. Plant Mol. Biol. 49: 199–214.

Kollmannsberger H, Fricke G, Paulus H & Nitz S (2000) The flavour composition of umbelliferous fruits. 1. Anise (*Pimpinella anisum*). Adv. Food Sci. 22: 47–61.

Kranz K & Petersen M (2003) β-Peltatin 6-*O*-methyltransferase from suspension cultures of *Linum nodiflorum.* Phytochemistry 64: 453–458.

Kraus C & Spiteller G (1997) Comparison of phenolic compounds from galls and shoots of *Picea glauca.* Phytochemistry 44: 59–67.

Kwon M, Burlat V, Davin LB & Lewis NG (1999) Localization of dirigent protein involved in lignan biosynthesis: implications for lignification at the tissue and subcellular level. In: Gross GG, Hemingway RW & Yoshida T (eds), Plant Polyphenols 2: Chemistry, Biology, Pharmacology, Ecology (pp. 393–411). Kluwer Academic/Plenum Publishers, New York.

Kwon M, Davin LB & Lewis NG (2001) *In situ* hybridization and immunolocalization of lignan reductases in woody tissues: implications for heartwood and other forms of vascular preservation. Phytochemistry 57: 899–914.

Lewis NG & Yamamoto E (1990) Lignin: occurrence, biogenesis and biodegradation. Annu. Rev. Plant Phys. Plant Mol. Biol. 41: 455–496.

Lewis NG & Davin LB (1992) Stereoselectivity in polyphenol biosynthesis. In: Hemingway RW & Laks PE (eds), Plant Polyphenols: Synthesis, Properties and Significance (pp. 73–95). Plenum Press, New York.

Lewis NG & Davin LB (1994) Evolution of lignan and neolignan biochemical pathways. In: Nes WD (ed) Isopentenoids and Other Natural Products: Evolution and Function, Vol 562 (pp. 202–246). ACS Symposium Series, Washington, DC.

Lewis NG, Kato MJ, Lopes N & Davin LB (1995) Lignans: diversity, biosynthesis and function. In: Seidl RS, Gottlieb OR & Kaplan MAC (eds), Chemistry of the Amazon: Biodiversity, Natural Products, and Environmental Issues, Vol 588 (pp. 135–167). ACS Symposium Series, Washington, DC.

Lewis NG & Davin LB (1998) The biochemical control of monolignol coupling and structure during lignan and lignin biosynthesis. In: Lewis NG & Sarkanen S (eds), Lignin and Lignan Biosynthesis, Vol 697 (pp. 334–361). ACS Symposium Series, Washington, DC.

Lewis NG, Davin LB & Sarkanen S (1998) Lignin and lignan biosynthesis: distinctions and reconciliations. In: Lewis NG & Sarkanen S (eds), Lignin and Lignan Biosynthesis, Vol 697 (pp. 1–27). ACS Symposium Series, Washington, DC.

Lewis NG & Davin LB (1999) Lignans: biosynthesis and function. In: Barton Sir DHR, Nakanishi K & Meth-Cohn O (eds), Comprehensive Natural Products Chemistry, Vol 1 (pp. 639–712.). Elsevier, London.

Lewis NG, Davin LB & Sarkanen S (1999) The nature and function of lignins. In: Barton Sir DHR, Nakanishi K & Meth-Cohn O (eds), Comprehensive Natural Products Chemistry, Vol 3 (pp. 617–745). Elsevier, London.

Li S, Iliefski T, Lundquist K & Wallis AFA (1997) Reassignment of relative stereochemistry at C-7 and C-8 in arylcoumaran neolignans. Phytochemistry 46: 929–934.

Lin RC, Skaltsounis AL, Seguin E, Tilleguin F & Koch M (1994) Phenolic constituents of *Selaginella doederleinii.* Planta Med. 60: 168–170.

Lundgren LN, Shen Z & Theander O (1985) The constituents of conifer needles. Dilignol glycosides from *Pinus massoniana* Lamb. Acta Chem. Scand. 39: 241–248.

MacRae WD & Towers GHN (1984) Biological activities of lignans. Phytochemistry 23: 1207–1220.

Mansell RL, Gross GG, Stöckigt J, Franke H & Zenk MH (1974) Purification and properties of cinnamyl alcohol dehydrogenase from higher plants involved in lignin biosynthesis. Phytochemistry 13: 2427–2435.

Marchand PA, Kato MJ & Lewis NG (1997a) (+)-Episesaminone, a *Sesamum indicum* furofuran lignan. Isolation and hemisynthesis. J. Nat. Prod. 60: 1189–1192.

Marchand PA, Zajicek J & Lewis NG (1997b) Oxygen insertion in *Sesamum indicum* furanofuran lignans. Diastereoselective syntheses of enzyme substrate analogues. Can. J. Chem. 75: 840–849.

Martin ME, Haourigui M, Pelissero C, Benassayag C & Numez EA (1996) Interactions between phytoestrogens and human sex steroid binding protein. Life Sci. 58: 429–436.

Min T, Kasahara H, Bedgar DL, Youn B, Lawrence PK, Gang DR, Halls SC, Park H, Hilsenbeck JL, Davin LB, Lewis NG & Kang CH (2003) Crystal structures of pinoresinol-lariciresinol and phenylcoumaran benzylic ether reductases, and their relationship to isoflavone reductases. J. Biol. Chem. 278: 50714–50723.

Mitski T, Thorne G & Lewis NG (2001) Patent: 'Plants having enhanced lignan synthesis' U.S. Provisional Patent Application filed April 9, 2001.

Moinuddin SGA, Hishiyama S, Cho M-H, Davin LB & Lewis NG (2003) Synthesis and chiral HPLC analysis of the dibenzyltetrahydrofuran lignans, larreatricins, 8′-*epi*-larreatricins, 3,3′-didemethoxyverrucosins and *meso*-3,3′-didemethoxynectandrin B in the creosote bush (*Larrea tridentata*): evidence for regiospecific control of coupling. Org. Biomol. Chem. 1: 2307–2313.

Molog GA, Empt U, Kuhlmann S, van Uden W, Pras N, Alfermann AW & Petersen M (2001) Desoxypodophyllotoxin 6-hydroxylase, a cytochrome P450 monooxygenase from cell cultures of *Linum flavum* involved in the biosynthesis of cytotoxic lignans. Planta 214: 288–294.

Mousavi Y & Adlercreutz H (1992) Enterolactone and estradiol inhibit each other's proliferative effect on MCF-7 breast cancer cells in culture. J. Steroid Biochem. Molec. Biol. 41: 615–619.

Nascimento IR & Lopes LMX (1999) 2,3-Dihydrobenzofuran neolignans from *Aristolochia pubescens.* Phytochemistry 52: 345–350 (and 53: 621).

Nascimento IR, Lopes LMX, Davin LB & Lewis NG (2000) Stereoselective synthesis of 8,9-licarinediols. Tetrahedron 56: 9181–9193.

Neidigh KA, Kingston DGI & Lewis NG (1994) Synthesis of stereospecifically deuterated matairesinol, podorhizol, epipodorhizol and yatein. J. Nat. Prod. 57: 791–800.

Nichols CR (2001) Chemotherapy of disseminated germ cell tumors. World J. Urol. 19: 82–89.

Nishibe S, Sakushima A, Kitagawa S, Klimek B, Benecke R & Thieme H (1988) Phenolic compounds from *Forsythia* leaves. III. On the comparison of constituents between hybrid and parents. Shoyakugaku Zasshi 42: 324–328.

Nose M, Bernards MA, Furlan M, Zajicek J, Eberhardt TL & Lewis NG (1995) Towards the specification of consecutive steps in macromolecular lignin assembly. Phytochemistry 39: 71–79.

Okunishi T, Umezawa T & Shimada M (2001) Isolation and enzymatic formation of lignans of *Daphne genkwa* and *Daphne odora.* J. Wood Sci. 47: 383–388.

Ozawa S, Davin LB & Lewis NG (1993) Formation of (−)-arctigenin in *Forsythia intermedia.* Phytochemistry 32: 643–652.

Paré PW, Wang H-B, Davin LB & Lewis NG (1994) (+)-Pinoresinol synthase: a stereoselective oxidase catalysing 8,8′-lignan formation in *Forsythia intermedia.* Tetrahedron Lett. 35: 4731–4734.

Pasini F, Durante E, De Manzoni D, Rosti G & Pelosi G (2002) High-dose chemotherapy in small-cell lung cancer. Anticancer Res. 22(6B): 3465–3472.

Patra A & Mitra AK (1979) Constituents of *Acorus calamus* Linn. Ind. J. Chem. 17B: 412-414.

Pullockaran AJ, Kingston DGI & Lewis NG (1989) Synthesis of stereospecifically deuterated desoxypodophyllotoxins and ^{1}H NMR assignment of desoxypodophyllotoxin. J. Nat. Prod. 52: 1290–1295.

Reichling J, Kemmerer B & Sauer-Gürth H (1995a) Biosynthesis of pseudoisoeugenols in tissue cultures of *Pimpinella anisum.* Pharm. World Sci. 17: 113–119.

Reichling J, Martin R & Kemmerer B (1995b) Biosynthesis of pseudoisoeugenol-derivatives in liquid tissue cultures of *Pimpinella anisum.* Plant Cell Tissue Org. Cult. 43: 131–136.

Rickard SE, Yuan YV & Thompson LU (2000) Plasma insulin-like growth factor I levels in rats are reduced by dietary supplementation of flaxseed or its lignan secoisolariciresinol diglycoside. Cancer Lett. 161: 47–55.

Sakakibara A, Sasaya T, Miki K & Takahashi H (1987) Lignans and Brauns' lignins from softwoods. Holzforschung 41: 1–11.

Sandler AB (2003) Chemotherapy for small cell lung cancer. Sem. Oncol. 30: 9–25.

Satake T, Murakami T, Saiki Y & Chen C-M (1978) Chemische Untersuchungen der Inhaltsstoffe von *Pteris vittata* L. Chem. Pharm. Bull. 26: 1619–1622.

Seidel V, Windhövel J, Eaton G, Alfermann AW, Arroo RRJ, Medarde M, Petersen M & Woolley JG (2002) Biosynthesis of podophyllotoxin in *Linum album* cell cultures. Planta 215: 1031–1039.

Stöckigt J & Klischies M (1977) Biosynthesis of lignans. Part I. Biosynthesis of arctiin and phillyrin. Holzforschung 31: 41–44.

Su W-C, Fang J-M & Cheng Y-S (1995) Flavonoids and lignans from leaves of *Cryptomeria japonica.* Phytochemistry 40: 563–566.

Susuki S, Umezawa T & Shimada M (1998) Stereochemical difference in secoisolariciresinol formation between cell-free extracts from petioles and from ripening seeds of *Arctium lappa* L. Biosci. Biotech. Biochem. 62: 1468–1470.

Susuki S, Umezawa T & Shimada M (1999) Stereochemical selectivity in secoisolariciresinol formation by cell-free extracts from *Arctium lappa* L. ripening seeds. Wood Res. 86: 37–38.

Susuki S, Sakakibara N, Umezawa T & Shimada M (2002a) Survey and enzymatic formation of lignans of *Anthriscus sylvestris.* J. Wood Sci. 48: 536–541.

Susuki S, Umezawa T & Shimada M (2002b) Stereochemical diversity in lignan biosynthesis of *Arctium lappa* L. Biosci. Biotech. Biochem. 66: 1262–1269.

Taniguchi E, Imamura K, Ishibashi F, Matsui T & Nishio A (1989) Structure of the novel insecticidal sesquilignan, Haedoxan A. Agric. Biol. Chem. 53: 631–643.

Tazaki H, Adam K-P & Becker H (1995) Five lignan derivatives from *in vitro* cultures of the liverwort *Jamesoniella autumnalis.* Phytochemistry 40: 1671–1675.

Teoh KH, Ford JD, Kim M-R, Davin LB & Lewis NG (2003) Delineating the metabolic pathway(s) to secoisolariciresinol diglucoside hydroxymethyl glutarate oligomers in flaxseed (*Linum usitatissimum*). In: Thompson LU & Cunnane SC (eds), Flaxseed in Human Nutrition, 2nd edition (pp. 41–62). AOCS Press, Champaign, IL.

Thompson LU, Rickard SE, Orcheson LJ & Seidl MM (1996a) Flaxseed and its lignan and oil components reduce mammary tumor growth at a late stage of carcinogenesis. Carcinogenesis 17: 1373–1376.

Thompson LU, Seidl MM, Rickard SE, Orcheson LJ & Fong HHS (1996b) Antitumorigenic effect of a mammalian lignan precursor from flaxseed. Nutr. Cancer 26: 159–165.

Thompson LU (1998) Experimental studies on lignans and cancer. Baillière's Clinical Endocrinology and Metabolism 12: 691–705.

Umezawa T, Davin LB & Lewis NG (1990a) Formation of the lignan (−)-secoisolariciresinol by cell-free extracts of *Forsythia intermedia.* Biochem. Biophys. Res. Commun. 171: 1008–1014.

Umezawa T, Davin LB, Yamamoto E, Kingston DGI & Lewis NG (1990b) Lignan biosynthesis in *Forsythia* species. J. Chem. Soc. Chem. Commun.: 1405–1408.

Umezawa T, Davin LB & Lewis NG (1991a) Formation of lignans, (−)-secoisolariciresinol and (−)-matairesinol, with *Forsythia intermedia* cell-free extracts. J. Biol. Chem. 266: 10210–10217.

Umezawa T, Davin LB & Lewis NG (1991b) Formation of optically pure lignans by cell-free extracts of *Forsythia intermedia.* In: Proceedings of the 35th Lignin Symposium, Tokyo, Japan, (pp. 33–36).

Umezawa T, Kuroda H, Isohata T & Shimada M (1992) Enantioselective lignan formation by cell-free extracts of *Forsythia koreana.* In: Proceedings of the 37th Lignin Symposium, Tokyo, Japan, (pp. 61–64).

Umezawa T, Kuroda H, Isohata T, Higuchi T & Shimada M (1994) Enantioselective lignan synthesis by cell-free extracts of *Forsythia koreana.* Biosci. Biotech. Biochem. 58: 230–234.

Umezawa T & Shimada M (1996) Formation of the lignan (+)-secoisolariciresinol by cell-free extracts of *Arctium lappa.* Biosci. Biotech. Biochem. 60: 736–737.

Vander Mijnsbrugge K, Beeckman H, De Rycke R, Van Montagu M, Engler G & Boerjan W (2000) Phenylcoumaran benzylic ether reductase, a prominent poplar xylem protein, is strongly associated with phenylpropanoid biosynthesis in lignifying cells. Planta 211: 502–509.

Wada H, Kido T, Tanaka N, Murakami T, Saiki Y & Chen C-M (1992) Chemical and chemotaxonomical studies of ferns. LXXXI. Characteristic lignans of Blechnaceous ferns. Chem. Pharm. Bull. 40: 2099–2101.

Wang C-Z, Davin LB & Lewis NG (2001) Stereoselective phenolic coupling in *Blechnum spicant*: formation of 8–2′ linked (−)-*cis*-blechnic, (−)-*trans*-blechnic and (−)-brainic acids. J. Chem. Soc. Chem. Commun.: 113–114.

Watanabe N, Sasaya T & Ozawa S (1992) Extractives of the genus *Corylus.* I. Lignans from the wood of *Corylus sieboldiana* blume. Mokuzai Gakkaishi 38: 796–803.

Xia Z-Q, Costa MA, Proctor J, Davin LB & Lewis NG (2000) Dirigent-mediated podophyllotoxin biosynthesis in *Linum flavum* and *Podophyllum peltatum.* Phytochemistry 55: 537–549.

Xia Z-Q, Costa MA, Pélissier HC, Davin LB & Lewis NG (2001) Secoisolariciresinol dehydrogenase purification, cloning and functional expression: implications for human health protection. J. Biol. Chem. 276: 12614–12623.